

THE IMACS CLUSTER BUILDING SURVEY:  
4. SPECTRAL EVOLUTION OF GALAXIES IN THE EPOCH OF CLUSTER ASSEMBLY \*

ALAN DRESSLER<sup>1</sup>, AUGUSTUS OEMLER<sup>1</sup>, BIANCA M. POGGIANTI<sup>2</sup>, MIKE GLADDERS<sup>3</sup>, BENEDETTA VULCANI<sup>2,4</sup>, LOUIS ABRAMSON<sup>3</sup>,

(Draft July 22, 2012)

ABSTRACT

Testing The *IMACS* Cluster Building Survey (ICBS) provides spectra of  $\sim 2200$  galaxies  $0.31 < z < 0.54$  in 5 rich clusters ( $R \lesssim 5$  Mpc) and the field. Infalling, dynamically cold groups of typically  $\sim 10$ -20 members account for approximately half of the supercluster population, contributing to a growth in cluster mass of  $\sim 100\%$  by today. The ICBS spectra distinguish non-starforming (PAS) and poststarburst (PSB) from starforming galaxies — continuously starforming (CSF) or starbursts, (SBH or SBO), identified by anomalously strong  $H\delta$  absorption or [O II] emission. For the infalling cluster groups and similar field groups, we find a correlation between PAS+PSB fraction and group mass, indicating substantial “preprocessing,” i.e., *quenching* mechanisms that can turn starforming galaxies into passive galaxies without the unique environment of rich clusters. Active starburst galaxies are common, and they maintain a constant ratio (SBH+SBO/CSF)  $\approx 1:4$  in all environments — from field, to groups, to rich clusters. Similarly, while PSB galaxies strongly favor denser environments, PSB/PAS  $\approx 1:10$  for all environments. This result, and their timescale  $\tau \sim 500$  Myr, indicates that starbursts are not signatures of a quenching mechanism(s) that produce the majority of passive galaxies. We suggest instead that starbursts and poststarbursts signal minor mergers and accretions, in starforming and passive galaxies, respectively, and that the principal mechanisms for producing passive systems are (1) early major mergers, for elliptical galaxies, and (2) late processes that turn spiral galaxies into S0’s — environment-dependent mechanisms such as starvation and stripping.

*Subject headings:* galaxies: clusters: general — galaxies: evolution — galaxies: groups: general  
galaxies: high-redshift — galaxies: star formation — galaxies: stellar content

1. INTRODUCTION

The *IMACS* Cluster Building Survey, ICBS, has used the wide-field multislit spectroscopic capability of the *IMACS* instrument on Baade-Magellan to map and study the galaxy populations of growing clusters at  $z \sim 0.5$ . One aim of the ICBS has been to learn whether the starburst activity seen prominently in the cores of rich clusters at this epoch is solely or at least primarily associated with the dense environment of a cluster core, or whether instead this activity is more widespread and associated in some way with the infalling population that is building the cluster.

In this paper we present classification and analysis of a large subset of the ICBS survey that includes spectrometric data on 1073 galaxies in five rich clusters covering the redshift range  $0.31 < z < 0.54$ , and 1091 galaxies covering the same redshift range that are members of the “field.” As described in Oemler et al. (2012a, Paper 1), the spectra from the approximately 30 multislit exposures with *IMACS* and *LDSS* were measured for spectral features and indices that quantitatively discriminate the degree and character of star formation in these galaxies. In addition to these data, separate measurements of  $H\alpha$  fluxes and, for two of the four fields, Spitzer-MIPS

$24\mu\text{m}$  fluxes were available to provide measures of star formation rates that are less sensitive to dust extinction.

Our goals here are two-fold: first, to assign spectral types to these galaxies based on the spectrophotometric measures, and second, to associate these with the larger-scale structures of groups and clusters in these fields. If possible, we hope to identify aspects of spectral evolution that can be connected to the environments in which they are found, whether or not that link is causative. Such information will help decide to what extent the star formation histories of these galaxies are influenced by their present environment, or predestined from their early environment, and possibly identify mechanisms that might be responsible in these regimes.

In §2 we describe the separation of the spectra into 5 spectral types, the distributions of other fundamental galaxy properties for these types, and the spatial distribution as described by the correlation of spectral type with local galaxy density and radial distance from a cluster center, and with the angular correlation function. In §3 we used the redshift data in these fields to identify moderate-sized, cold groups infalling into clusters, and to identify comparable groups and filaments in the field, and we describe the basic properties of these groups. In §4 we use spectral types and spatial/structural information to discuss the evidence for quenching processes that turn starforming into passive galaxies across the full range of environments from isolated galaxies to rich cluster cores, and explore the connection of starburst galaxies to the quenching process, developing a model that could account for the wide range of data that describe star for-

\*This paper includes data gathered with the 6.5 meter Magellan Telescopes located at Las Campanas Observatory, Chile.

<sup>1</sup> The Observatories of the Carnegie Institution for Science, 813 Santa Barbara St., Pasadena, CA 91101, USA

<sup>2</sup> INAF-Astronomical Observatory of Padova, Italy

<sup>3</sup> Department of Astronomy and Astrophysics, University of Chicago, 5640 S. El St, Chicago, IL 60637, USA

<sup>4</sup> Astronomical Department, Padova University, Italy

mation histories across all galaxy environments.

## 2. STAR FORMATION HISTORIES FROM SPECTROPHOTOMETRIC DATA

### 2.1. Division into five spectral types

As described in Paper 1, the fields chosen for the ICBS were centered on putative rich clusters selected by the red-sequence method Gladders & Yee (2005). Catalogs from photometric observations with the duPont 2.5-m at Las Campanas Observatory were used to select objects for spectroscopic observations. A non-trivial combination of prioritizing objects by brightness and filling in multislit masks with any available galaxy resulted in a sample that is approximately magnitude-limited at Sloan  $r = 22.5$  with a tail to galaxies as faint as  $r = 23.5$ . A comparison of the incompleteness of the spectroscopic sample compared to the photometric source catalog is shown in Paper 1.

Our redshift survey of more than 1000 galaxies per field revealed 6 rich clusters, with the RCS1102 and SDSS1500 fields each containing two. In RCS1102, the serendipitous cluster at  $z = 0.2550$  is rich (157 members in our sample) and has a high velocity dispersion of  $\sigma_0 \approx 930$  km s<sup>-1</sup>, but the cluster is centered at the edge of our field or perhaps beyond, and the lower redshift means that key spectral features fell below the spectral window we used for most of the spectroscopy, so this cluster has been excluded from our sample. Basic parameters for remaining 5 clusters, including sample properties that apply specifically to this paper, are given in Table 1. Cluster members were chosen in an interval of rest frame velocity  $\pm 3000$  km s<sup>-1</sup>, which reasonably if not perfectly sequesters the cluster and its supercluster from the field (see Figure 16 of Paper 1). A field sample was selected for each sky field that covers the same redshift range as the 5 clusters,  $0.31 < z < 0.54$  — excluding, for each field, the  $z$ -range of the cluster(s), referred to as the *cl.field*.

The galaxies in the 5 cluster and 4 field samples were divided into five distinct spectral classes, based on star formation rate, the presence of Balmer absorption lines, and the broad-band rest-frame B-V color of each galaxy. As explained in Paper 1, star formation rate was measured in several ways, from 24 $\mu$ m luminosities and H $\alpha$ , H $\beta$ , and/or [O II] fluxes, using relationships that have been derived by others to convert these measurements, and using relationships that we derive, into star formation rates (SFRs) in solar masses per year. Because all three measures are not available for all galaxies in the sample, a prioritized system based on the expected accuracy of each method was adopted, also explained in Paper 1.

As first noted by Dressler & Gunn (1983) and quantified by Couch & Sharples (1987), strong Balmer absorption is usually indicative of a recent starburst in the star formation history of a galaxy. H $\delta$  is particularly well suited for this measurement, and a strong detection of H $\delta$  in what is otherwise an old K-giant type spectrum is a reliable sign of a poststarburst galaxy.<sup>5</sup> However, for a galaxy in which starformation is ongoing, it is important to recognize that stronger Balmer lines are also the

result of vigorous star formation. The ICBS has better quantified this effect by using well-studied local samples to define a relation between SFR and H $\delta$  absorption in the absence of star burst, as explained in Paper 1. Using this, we define a  $\Delta$ H $\delta$  index which measures the Balmer-line strength in excess of that expected in a continuously star forming system to identify with a starburst.

Finally, to better identify starbursts, we have revisited the issue of whether strong [O II] emission alone can signal a starburst, as introduced in Poggianti et al. 1999. Again, using local samples, we have determined that the fixed limit in equivalent width  $W_{eqw} > 40 \text{ \AA}$  used previously must be refined by using a limit that is a function of a galaxy’s specific star formation rate.

Using these measurements of star formation rates and optical line strengths, we define five spectral types as follows: (1) PAS (passive) — SFR  $\leq 0.0$  and  $\Delta$ H $\delta \leq 0.0$ ; (2) CSF (continuously starforming) — SFR  $> 0.0$  and  $\Delta$ H $\delta \leq 0.0$  and not [O II] starburst; SBH (starburst from H $\delta$ ) — SFR  $> 0.0$  and  $\Delta$ H $\delta > 0.0$  and not [O II] starburst; PSB (poststarburst) — SFR  $\leq 0.0$  and  $\Delta$ H $\delta > 0.0$ ; and SBO (starburst based on equivalent width of [O II]).

Extra attention was given to the of-order hundred objects with a marginal detection of star formation using one or more indicators, to determine which of these were in fact likely PAS galaxies. The spectra of these objects were examined closely to estimate the S/N of emission-lines [O II], H $\beta$ , [O III], and H $\alpha$ , and to determine whether the line-strength of any of these automatically-detected feature was at the sensitivity limit of the ICBS data. In general, if the starforming classification was based on a single determination of the SFR at the detection limit (a function of redshift), the classification was changed to PAS, while multiple detections of a non-zero SFR, even if at their detection limits, kept the galaxy in the starforming category. Although the boundary between PAS and star-forming cannot be sharp at the detection limit for these optical features and 24  $\mu$ m flux, the application of this criteria essentially divided ambiguous cases between PAS and starforming at a SFR of 1 M $_{\odot}$  yr<sup>-1</sup>, equivalent, for a galaxy in our sample, to a specific star formation rate, sSFR of 10<sup>-11</sup> yr<sup>-1</sup>. The distribution of these quantities is shown in the following section.

### 2.2. Galaxy properties of 5 spectral types

Before we consider the properties of this sample of “cluster” galaxies, we need to remind the reader that the samples discussed here are from much more extensive fields — about  $R \sim 5$  Mpc in radius — than are usually studied for either local or distant clusters of galaxies. The typical volume of investigation is a sphere of radius  $R \sim 1$ , approximately the virial radius and a few core radii. The ICBS fields are substantially larger. Furthermore, our sample is more incomplete, up to a factor of 2, in this core-cluster region, compared to  $\sim 80\%$  completeness throughout the rest of each field — this is the result of the crowding of the galaxies in the core regions, which could not be as well covered with the  $\sim 6$ -8 multi-slit masks we used to study each field. We have not corrected for incompleteness in the distributions presented in this section, which are intended only to show the distribution of the collected data in this volume that includes

<sup>5</sup> As explained in Paper 1, we use a modified measure of the H $\delta$  index in the ICBS which improves the measurement of Balmer line strength by including measurement of the (H+He)/K ratio.

the cluster core and the region of cluster infall. Although the galaxies infalling into the clusters are not part of the cluster core population at this epoch, we will confirm below that this is a region of infall that will substantially build the cluster during this epoch — the outer population we are studying will become part of the traditional cluster sample for a present-epoch cluster.

Figure 1a-d shows unweighted distributions in absolute magnitude  $M_B$ , rest-frame  $B - V$  color, galaxy mass, and star formation rate, respectively, for galaxies of the five spectral types in four of the clusters in the sample (solid histogram) and the cl\_field (open histogram). The cluster SDSS1500B is not included in these distributions because its higher redshift results in significant incompleteness for low-luminosity galaxies.

The distribution in absolute blue magnitude Figure 1-a shows little difference between the PAS and CSF subtypes: both the mean and the dispersion are very similar. While bearing in mind the difference in sampling just discussed, this contrasts to what is true for low-redshift cluster populations, where there is only a small percentage of starforming galaxies and with only rare examples as luminous as the brightest passive galaxies. This suggests that these galaxies, presumably starforming spirals, will need to fade substantially by  $\sim 1$  mag from the brightness observed here, or that the brightest starforming galaxies in particular have not survived as such.

The next thing to notice is that the three types associated with starbursts do not share this distribution of absolute brightness with the passive and continuously-star-forming populations. In particular, active starbursts selected by enhanced  $H\delta$  absorption — SBH — are less luminous, on average, by a factor  $\sim 2$ , than CSF types. Among other things, this demonstrates that this class is distinct from the CSFs — these are not simply CSFs with erroneous measurements of  $H\delta$ . SBO galaxies appear to be even less luminous, but the sample is small. The poststarbursts, PSB, appear to share the luminosity distribution of the active starbursts, although different levels of dust extinction could be partly responsible for the apparent similarity (as first suggested in Poggianti et al. 1999; see also Dressler et al. 2009b). However, the principal difference in these distributions of total blue magnitude is that all the starburst types lack systems as bright as the most luminous CSF galaxies. This may be instead a result of a selection effect — the difficulty of identifying starbursts in very luminous systems, an issue we discuss in §4.6.

The SBO are, if anything, fainter than the SBH, and our estimates of the extinction in these systems suggest that they are considerably less dusty than typical CSF. These objects, more typical of what has been traditionally identified as a starburst, were noted by Poggianti et al. as clearly too faint to feed brighter half of the PSB population, a conclusion that is born out as well in the new samples.

The effect of dust extinction is evident in the color distributions, Figure 1-b, and SFR distributions, Figure 1-d. The PAS are, of course, the reddest galaxies in the clusters, and their color dispersion is unsurprisingly small. Likewise, the CSF span a very wide range of colors, although there are few truly red galaxies, again, as expected. The SBH are slightly bluer, on average, than the CSF, but not as blue as expected for such starbursts.

This can be attributed to dust: if the SBH had a normal amount of dust, they would be considerably bluer than the CSF, as would be expected for their higher star formation rates of many solar masses per year (see Figure 1-d). The SBO are the bluest sample, consistent with their high rates of star formation and lower dust contents.

Figure 1-c shows the stellar mass distribution for the 5 spectral types. Despite their similar  $M_B$  distributions, PAS are, on average, more massive than CSF galaxies. SBH galaxies are on average a factor-of-two less massive than CSF galaxies, and SBO galaxies even less massive than these. These sample sizes are small, although again, the paucity of massive galaxies among the starburst types seems very clear, as it was for the  $M_B$  distribution.

The SFR for sptypes CSF, SBH, and SBO is shown in Figure 1-d. It is important to explain that, although the latter are clearly starbursts, their SFRs largely overlap with the SFRs of CSF galaxies. This is because the definition of a starburst is related to the rise in the SFR over  $\sim 10^8$  years compared to the past average, a factor of 3-10 for the starburst galaxies in the ICBS sample, for galaxies which range in mass by a factor of 100. In order to see evidence for a higher SFR than a comparable CSF galaxy, then, it is necessary to normalize by the mass — the specific star formation rate (sSFR) shown in the bottom half of Figure 1-d. Here we see that the SBH types have a smaller range of sSFR than the CSF and also a mean sSFR a factor-of-two greater. Notably, the distribution of sSFR for SBO galaxies is, if anything, broader than the CSF distribution, and the mean sSFR of SBO galaxies is a factor-of-4 higher, consistent with (though no sufficient for) their identification as starbursts.

Conspicuous in Figure 1-d is the fact that the SBH do not include sSFR's that are as high as the CSF, which would seem to raise some doubt as to whether they are starbursts while galaxies with higher sSFR are not. However, this can be understood by remembering that a galaxy can have a high sSFR without a burst if it is efficiently forming stars for a several Gyr period of the recent past and did not form the bulk of its stars within the first few Gyr of cosmic history. A galaxy with a star formation history more weighted to early epochs cannot reach such high values of sSFR because of the higher mass accumulated in early epochs. Our use of spectral features to quantify the time scale of the SBH and SBO phases and is able to distinguish galaxies that are forming stars very efficiently over a several Gyr period before the epoch of observation from those in which an increase in “efficiency” is a more recent, temporary condition that we identify as a moderate starburst.

As mentioned above, the completeness of detected star formation falls rapidly below an SFR of  $1 M_\odot \text{ yr}^{-1}$ , or a sSFR of  $10^{-11} \text{ yr}^{-1}$ , for the typical galaxies of the ICBS sample. The inspection procedure described attempts to include SFRs that are lower than these limits but are nevertheless reliable detections — cases of unusually good spectra or two or more marginal detections that exceed the typical detection limits.

### 2.3. *The spatial distribution of galaxies of the five spectral types*

Figure 2 shows the distribution of spectral types in the 5 clusters in the 4 fields. We again recall that these are

more extensive fields, about 10 Mpc in diameter, than are typically studied around distant clusters of galaxies. The typical volume studied in an intermediate-redshift rich cluster is  $\sim 2$  core radii, is contained in a sphere of radius  $R \sim 0.5$  Mpc, about  $0.03^\circ$  for the clusters in this sample. In comparison with the virial radius (which we calculate in the conventional way as  $r_{200}$ , we see from Table 1 that typically  $R_{vir} \approx 1.3$  Mpc, about  $0.07^\circ$ , still a small fraction of the  $R < 0.45^\circ$  field of *IMACS*.

With this in mind, several things are nevertheless readily apparent from the plots of Figure 2. All five fields show large numbers of galaxies within the redshift range of the cluster (defined here as  $\Delta V < \pm 3000$  km s $^{-1}$  in the rest frame from the cluster systemic velocity), that is, there is not a sharp falloff in supercluster members but more of a shelf-like distribution. Furthermore, in four of the five fields, there appear to be a substantial clumping of these galaxies. Only SDSS0845A, shown in the center of Figure 2, appears to show the relatively uniform halo of galaxies typical of rich, present-epoch clusters like Abell 1656 (Coma), Abell 2199, or Abell 2029. Indeed, there is very high degree of real substructure in the form of infalling groups in these fields, which we will show in the §3.

We begin by considering the distributions of the two most populous spectral types, PAS and CSF. It is clear just from casual visual inspection of the figures that passive galaxies are found preferentially in the high-density cluster cores. Echoing the morphology/local-density relation, we expect these to be morphological types E & S0 galaxies (Dressler et al. 1999; Postman et al. 2005). Similar to the distribution of morphological spiral galaxies in the small number of intermediate-redshift clusters imaged with large mosaics of HST images, the spectral-type CSF galaxies dominate the lower density halo of the cluster, for the most part avoiding the dense cores entirely. In fact, we can derive a spectral-type/surface-density relation for these data that quantifies this likely association, which we show in Figure 3. The qualitative, even quantitative resemblance of this diagram with the morphology-density relation reinforces the idea that these spectral types correspond well with the galaxy morphologies found for such spectra at the present epoch. Figure 3 also shows that the spectra-type/radial-distance relation is quite similar to the spectral-type/density relation for the three more-or-less regular clusters RCS0221A, RCS1102B, and SDSS0845A, but that the sptype/density relation appears stronger for the two more irregular clusters, SDSS1500A & B, where the spectral-type/radial-distance relation is absent outside the two points representing the cluster cores. As with the relations for morphology, these results suggest that, to the extent that passive galaxies descend from star forming galaxies, the processes responsible are more likely related to local density over the lifetime of galaxies, rather than processes that are “global” in the sense that they are due to the properties of the cluster itself, for example, the tidal field or hot intercluster gas. We will, however, return to this long-standing question in §4.

Returning to Figure 2 to consider the distribution of spectral types associated with starbursts, we see that the PSB galaxies are in fact very much distributed like the PAS galaxies, that is, favoring dense cluster cores or density enhancements of groups, for example, the lower left

corner of SDSS1500B. However, the active starbursts, both SBH and SBO, are spread throughout the clusters with no obvious affinity for denser regions, indeed, they seem to share the distribution of the CSF galaxies, as if they derive from the same population. This effect also shows up very clearly in the sptype/surface-density relation of Figure 3 (bottom), where the active starburst fraction rises and the poststarburst fraction falls with increasing galaxy local-surface-density.

We quantify these effects further in Figure 4, where we show the angular auto-correlation functions of PAS galaxies and cross-correlation functions of the other spectral types with the PAS galaxies. Again we have divide the sample between (a) the three more regular clusters and (b) the two less regular ones. The PAS autocorrelation function is strongest, reflecting their concentration to smaller, dense regions. What is somewhat remarkable, however, is the strength of the PSB cross-correlation: these galaxies are as strongly clustered as the PAS galaxies, which means that the PSB must in fact share the spatial distribution to high fidelity. This correspondence of PAS and PSB distributions is clearly seen in both the regular and less-regular clusters – in Figure 4-a and -b.

When we compare the spatial distribution of CSF and active starbursts, SBH+SBO galaxies, our visual impression from Figure 2 is confirmed: the close correspondence of the autocorrelation functions for the active starburst galaxies with the CSF strongly suggest that the former are a “random” draw from the latter, in other words, any of the CSF galaxies appear to be candidates for a starburst.

The remarkable way in which the PSB spatial distribution traces the PAS distribution, and the SBH+SBO spatial distribution traces the CSF distribution, while the PAS and CSF spatial distributions are so different, suggest that there is more than a casual connection between starforming/passive and starburst/poststarburst spectral types. A simple picture where some or all of the active starbursts are becoming poststarbursts, perhaps on their way to becoming PAS galaxies, seems inconsistent with this picture. Indeed, in §4 we shall provide other evidence that this PSB-PAS and (SBH+SBO)-CSF connection holds in other environments than rich clusters and their superclusters, a clue to an alternate picture that we discuss in §4.

### 3. THE STRUCTURAL EVOLUTION OF THE ICBS CLUSTERS

It is a feature of N-body models of hierarchical structure building to show the evolution of rich clusters as the result of intersecting regions of high density, specifically, the intersection of galaxy filaments and sheets where galaxies are channeled into regions of highest density. One of the motivations of the ICBS was to search for evidence of this effect, which the simulations indicate is strong at intermediate redshift.

#### 3.1. *The identification of infalling groups*

It is clear from inspecting the maps in Figure 2 that filamentary structures are not so obvious in projection to allow a simple spatial selection of structures that might be involved in building these clusters. Because of this, we chose to use the Dressler & Shectman (1988) subclus-

tering test (DS-test) as a tool for identifying structures that are kinematically distinct from the high-velocity dispersion environment that characterizes the cluster as a whole. As used here, the test identifies dynamically cold structures by finding the 10 nearest galaxies (in the spectroscopic sample) and comparing the velocity dispersion and systemic velocity for each such subset to the velocity dispersion and systemic velocity for the cluster as a whole. A “sum-of-squares” deviation  $\delta$  is calculated for each galaxy; these values are not independent, obviously, and they do not identify groups uniquely, but the point clearly to areas where physical groups can be found.

In the Dressler-Shectman study, the test was only used to demonstrate the statistical significance of subclustering. A  $\Delta$  parameter was calculated by the root-mean-square of the individual  $\delta$  values, and this was compared to the results of a large number of simulated clusters made by randomly shuffling the velocities between galaxies in order to estimate the significance of that  $\Delta$  value.

Because the DS-test does not find groups per se, and the individual  $\delta$  deviations are not at all independent, the DS-test is by itself insufficient for the purpose here. However, we found that, by calculating and plotting the  $\delta$  deviations for each galaxy in the field, the test very reliably found places where groups could be found; it was then a straightforward matter to investigate galaxy-by-galaxy whether discrete groups – based on association of their redshifts – could be found. In practice, this turned out to be surprisingly easy to accomplish.

In Figures 5 – 7 we present the elements of the procedure we used to identify and quantify the properties of the groups. For each cluster, we ran the DS-test and found the areas where deviations from the global cluster values of velocity and velocity dispersion are large. These are shown at the top of the panel for each cluster. The points are scaled by the size of the  $\delta$  deviation for each galaxy with its 10 neighbors, so big circles indicate large deviations. Using this as a map, we selected all objects within the area bounded by the big circles, and plotted their velocities relative to the cluster mean. In almost every case a single or double peak of low velocity dispersion ( $\sigma \lesssim 350 \text{ km s}^{-1}$ ) was found; the number of galaxies outside of these relatively cold structures was always much smaller than those inside. This made it unambiguous to eliminate them from the trial groups. A second pass was made around the perimeter of each group to see if the group extended further in any direction (the sensitivity of the DS-test falls as more non-deviant objects are among the 10 neighbors), but usually there were at most a few additional objects that fit well into the groups. In practice, the number of objects added to the groups by exploring the perimeter was  $\lesssim 20\%$  of those originally identified. Because of this, the process rapidly covered — the groups never had to be redefined after this step.

The groups identified in this manner are shown in the middle map of each panel, with the groups identified by symbols and color. Velocity histograms of the identified groups are shown in the bottom plot of each panel. The group in the upper left corner of RCS1102B, Group 2, is an example of one where there is almost no contamination by non-group members – compared to the 15 group members found, only 2 galaxies in the area lay outside the well defined velocity histogram Figures 5-f. RCS0221A – 1A and 1B are not well separated from the

main body of the cluster, yet here again, only 7 galaxies had to be excluded to form these two groups of 20 and 16 members respectively, which separate distinctly in the velocity histograms, Figure 5-c.

### 3.2. Properties of the groups

The basic parameters of each of the groups are given in Table 2. Groups were divided into A & B if two different velocity structures were found co-located in projected space. There are 5, 6, 5, and 6 groups identified for RCS0221A, RCS1102B, SDSS1500A, and SDSS1500B, respectively. Only 2 groups are found for the rich, regular cluster SDSS0845A, and one of these is well beyond the  $3000 \text{ km s}^{-1}$  (rest-frame) velocity limit of a candidate for infall – this and group 1B in SDSS1500B are assumed to be projections of groups that are at least  $\sim 40$  Mpc in front of the cluster (discounting the possibility of non-Hubble velocities that are more than  $3000 \text{ km s}^{-1}$ ). However, the remaining 23 groups are all candidates for delivering future cluster members, even though the infall velocities of a few are as high as  $\sim 2500 \text{ km s}^{-1}$  in projection. This is shown in Figure 10, where the velocities of all galaxies in the groups are compared to the remaining cluster members. It is clear that the group members trace the same velocity distribution as the cluster members, that is, they are sampling the same gravitational potential. Without a doubt, these groups are delivering the next wave of cluster members.

To test the statistical significance of these groups, we made Monte Carlo tests based on the overall velocity distribution in the field, that is, we asked, for a group of  $N$  members, how often  $N$  random draws from the global velocity distribution yield a velocity dispersion as small, or smaller, than the measured velocity dispersion of that group. To be faithful to the procedure used in picking the groups, we allowed the program actually pick  $N + N_{\text{ex}}$  members, where  $N_{\text{ex}}$  is the number of excluded galaxies within the bounded region of the group, and form the lowest velocity-dispersion group of  $N$  members from that sample (like making the best 5-card poker hand from 7 dealt cards). Table 2 contains the  $N_{\text{ex}}$  values for each group and the derived probability of randomly concocting such a group at any location in the cluster. The groups were found to be highly significant, with a typical probability of  $10^{-3}$ : 22 of the 24 groups have probabilities  $P \lesssim 1\%$ . SDSS1500A group 2 has a near-zero difference from the systemic velocity of the cluster, and with only 6 members its  $200 \text{ km s}^{-1}$  velocity dispersion could be a random draw 16% of the time, according to the Monte Carlo test. It is, nevertheless compact, and isolated, so it is likely to be a real subgroup. SDSS1500B group 2 is more interesting: it has a high probability of being a random selection from the cluster velocity distribution, 23%, but this is because it is as hot as the cluster ( $\sigma_0 = 915 \text{ km s}^{-1}$ ) at essentially the cluster systemic velocity ( $\Delta V_0 = -100 \text{ km s}^{-1}$ ). There is no doubt that this is a dynamical group, however, as it has 29 members with an effective radius of 0.7 Mpc, a remarkable structure that is denser than the SDSS1500B cluster core. We discuss this rich group further in the next section.

All of the groups share basic morphological features – they all are roughly round in shape rather than filamentary. Although we had expected to see filaments

like those in the N-body simulations, it could be that our fields, though large, still do not extend far enough to reach these filaments. Regardless, our finding of many infalling groups that are well bounded and essentially round suggests that, if filaments are feeding the growth of these clusters, the formation of such groups would have to come from these further-out filaments. The typical group has 10-20 members, an effective radius of 1 Mpc, and a velocity dispersion of  $250 \text{ km s}^{-1}$ . In addition to the homogeneity of the cluster groups, however, there are a few interesting cases that we now describe.

1. RCS0221A group 1A and 1B appear to cover the same kidney-bean shaped region on the sky, yet they appear kinematically distinct with a relative velocity difference of  $\sim 2000 \text{ km s}^{-1}$ . The same appears to be true for RCS0221A groups 2A and 2B, but it is also possible that they are part of a single velocity distribution. RCS1102B group 1A and 1B may similarly be from a single, though very asymmetric, velocity distribution.
2. RCS1102B group 5 is extremely compact ( $R_{\text{pair}} = 0.14 \text{ Mpc!}$ ), relatively cold ( $\sigma_0 = 335 \text{ km s}^{-1}$ ) and has a high relative velocity of  $-843 \text{ km s}^{-1}$  (rest-frame) with respect to the cluster mean. This would seem to be a small clump or filament that is falling in from the backside or has fallen through the core. The spectral type distribution is 60% PAS, 20% CSF, and 20% PSB, an unusually high poststarburst fraction. It is tempting to consider this a case of a strong environmental influence by the cluster core on an infalling group or line-of-sight filamentary structure.
3. SDSS1500A groups 4A & 4B are compact central concentrations or filament projected directly on the cluster core. It appears to break into two cold groups at  $+500 \text{ km s}^{-1}$  and  $-800 \text{ km s}^{-1}$  with respect to the cluster systemic velocity. Of its combined 20 members, 10 are PAS, with 3 active starbursts and 2 poststarbursts as well. As in the case of RCS1102B, a cluster-core-influence could be inferred.
4. SDSS1500B group 3 is another very compact structure projected against the cluster core. It has a high infall velocity ( $V_0 \approx 1500 \text{ km s}^{-1}$ ) from the frontside and is relatively hot,  $\sigma_0 \approx 500 \text{ km s}^{-1}$ , and 5 out of 8 members are PAS.

### 3.3. The identification of comparable groups in the field

The groups identified in the previous section are clearly providing a major, perhaps the dominant component in the building of these clusters. One of the goals of the ICBS is to look for evidence of spectral evolution in the infalling population to help understand what role, if any, is played by the cluster environment as distinct from that of the groups that have brought the cluster to this state of assembly. In order to address this issue, it is important to compare the properties of these supercluster groups to those of the general field. To accomplish this, we searched for and identified groups in the “cl.field” sample over the same redshift range as the cluster observations

with the goal of finding groups whose basic parameters — size, richness, and velocity dispersion — were similar to the cluster groups.

The results of an automatic “friends-of-friends” search (Paper 2) had already provided a catalog of small groups, but these were not a good match to the cluster sample. Because there is not a comparatively narrow redshift interval in this field sample as there is for each cluster, it is not straightforward to use the Dressler-Shectman test, which is based on the fact that all objects in the sample are members of the cluster. We therefore decided on a visual inspection of galaxies in “spikes” of the redshift distribution. This was accomplished by investigating  $\Delta z = 0.02$  slices, stepped in  $\Delta z = 0.01$  increments through the full depth. In order to match the cluster sample, where the dense cluster environment dominates over the central few megaparsecs of the field (leaving mainly the region outside this available for a group search), we concentrated on groups that were a few Mpc or smaller in projection on the sky, but our search turned up larger systems that had not been found in the clusters sample. A couple of field groups stretch across most of the *IMACS* field. Possibly, such large groups cannot survive in close proximity to a rich cluster.

The search yielded 30 groups, whose properties are listed in Table 3. Again, we found that this process was quite unambiguous: we generally found well defined structures with little confusion as to what was or was not a likely member. This is demonstrated by the size of the groups and their low velocity dispersions — 29 of the 30 groups have velocity dispersions  $\sigma < 350 \text{ km s}^{-1}$  and 18 of 30 have  $\sigma < 250 \text{ km s}^{-1}$ .

The morphology of most of these field groups overlapped that of the cluster groups, but a sizable minority have a narrow filamentary shape that was not found in the cluster sample. In Figure 8 we show these groups and filaments separately for the 4 fields. Histograms of basic group parameters are shown in Figure 12 and are discussed below.

## 4. DISCUSSION

### 4.1. Galaxy clusters under construction

It has been well recognized for the last two decades that clusters have grown through the accretion of systems of all scales, from single galaxies and moderate-sized groups to cluster-cluster mergers. Accordingly, finding substructure is an unsurprising result of any study of rich clusters. However, this point of view developed slowly in the 1980’s as substructure in clusters was recognized as the consequence of hierarchical structure growth, as first suggested by White (1977). Up to this time the prevailing view was that clusters, typified by the only very well-studied cluster Abell 1656 (Coma), had smooth, axially symmetric distributions of galaxies. This picture suggested a process of cluster formation that either did not involve merging or accretion of smaller structures, or a process that actually destroyed them, in particular, the Lynden-Bell (1967) “violent relaxation” model that described the gravitational collapse of a volume of roughly uniform density — an uncommon occurrence in a hierarchical universe.

Dressler’s (1980) discovery of a correlation between galaxy morphology and local projected density was re-

garded skeptically because “violent relaxation” was the prevailing picture of cluster formation: if apparent subgroups in clusters were merely statistical density fluctuations they would be too short-lived to be seriously involved in morphological evolution. In reviewing the observational data on substructure, and making the first quantitative estimate of the prevalence of substructure through surface-density contour maps, Geller & Beers (1982) found statistically significant substructure in  $\sim 40\%$  of a sample of 65 rich clusters studied by Dressler (1976, 1980), a necessary if not necessarily sufficient degree of subclustering to account for the morphology-density relation. As the number of available redshifts in such clusters grew, more discriminating tests became possible. Dressler & Shectman’s (1988) study, which employed the statistical test described above and used  $\sim 1000$  cluster redshifts divided among 15 of the same clusters, agreed, concluding that “In 30-40% of the cases, the subclusters contain a large fraction of the galaxies found in the main body of the cluster.”

Hierarchical clustering suggests that the clusters of the relatively recent past,  $0.3 < z < 1.0$  should exhibit much stronger substructure compared to present-epoch rich clusters (Kauffmann 1995), and indeed, observations have produced some striking examples (e.g., De Filipis & Schindler 2003; Kodama et al. 2005; Oemler et al. 2009). However, the selection of intermediate-redshift rich clusters for study has been badly biased to clusters with strong X-ray emission: at any epoch, these are the most dynamically evolved and exhibit the least amount of substructure. The ICBS includes one such cluster, SDSS0845, which is populous and has a smooth symmetric distribution; indeed, it includes only one small infalling group in the field (Figure 6-b), in contrast with the many infalling groups of each of the other 4 clusters. Furthermore, most studies of distant clusters, particularly those making use of HST imaging, cover relatively small volumes of space around intermediate-redshift clusters,  $R \lesssim 1$  Mpc, approximately the virial radius of clusters of this richness and therefore essentially the part of the cluster where substructure is more likely to have been erased.

For these reasons, we believe that the ICBS program may be the first to investigate this question of cluster growth for typical rich clusters over the required volume to see the infalling population that will be incorporated into the cluster between the redshift of observation and the present epoch. Our finding of a robust population of infalling groups of 10-20 members in 4 of the 5 clusters of our study, shown in Figures 5 and 7, may be in fact the most representative view to-date of how a typical rich cluster of today was assembled.

#### 4.2. Building Clusters Through Group or Galaxy Accretion?

The identification of kinematically distinct groups in the ICBS clusters offers the possibility of a quantitative test of the paradigm  $\Lambda$ CDM model (Springel et al. 2005). There are, of course, many subtleties involved in comparing easily identifiable galaxies in the sky to the dark matter halos that N-body simulations trace. The ICBS directly samples only about 1.6 Gyr of cosmic time: although we have argued that the ICBS clusters are typical clusters at this epoch in terms of the maturity of their

dynamical evolution, the infall we measure is limited to a few billion year interval of cluster history. For this reason, it is not straightforward to compare our results with apparently suitable theoretical studies on galaxy infall into clusters, for example, the  $\Lambda$ CDM N-body simulations by McGee et al. (2009), Berrier et al. (2009), and De Lucia et al. (2011). A principal motivation of these studies was to investigate whether so-called “pre-processing” in groups of galaxies — before the dense environment of the cluster is encountered — could produce the much larger fraction of passive galaxies in rich clusters, as opposed to cluster-specific processes such as ram-pressure stripping or starvation that operate most efficiently in the cluster environment.

Berrier et al. conclude that such preprocessing is not important:

“On average, 70% of cluster galaxies fall into the cluster potential directly from the field, with no luminous companions in their host halos at the time of accretion; less than 12% are accreted as members of groups with five or more galaxies.”

McGee et al. find essentially the opposite

“We find that clusters at all examined redshifts have accreted a significant fraction of their final galaxy populations through galaxy groups. A  $10^{14.5} h^{-1} M_{\odot}$  mass cluster at  $z = 0$  has, on average, accreted  $\sim 40\%$  of its galaxies ( $M_{\text{stellar}} > 10^9 h^{-1} M_{\odot}$ ) from halos with masses greater than  $10^{13} h^{-1} M_{\odot}$ .”

Confirming the conclusions of McGee et al., De Lucia et al. (2011) attribute the importance of distinguishing between different timescales of accretion into a group, as distinct from accretion into the final cluster, as important to reconciling the apparently different result of Berrier et al.

It is not obvious how to decide if these criteria are met by the ICBS infalling groups, or whether the conclusions of these theoretical studies refer only to virialized halos, which likely describes only some of the ICBS groups. Furthermore, the percentages given by these studies are averaged over some longer history of the cluster, while the ICBS samples a narrower epoch of the cluster’s growth. It is clear, however, than what we are observing at  $z \sim 0.5$  will substantially increase the cluster’s mass in the several gigayears required to incorporate the groups into the cluster, so at minimum an estimate of the fraction of galaxies in a group environment compared to single galaxies is needed to compare with model simulations.

For the four ICBS clusters RCS0221A, RCS1102B, SDSS1500A, and SDSS1500B, 257 galaxies have been identified as members of the 24 groups, compared to 532 cluster members that are not members of groups. This means that the mass of these clusters will grow by at least  $\sim 50\%$  by the present epoch. (This compares to less than  $\sim 7\%$  for the minimum growth of SDSS0845, an already relaxed, concentrated cluster, based on the single infalling group we identified.) However, these must be lower-limits, because it is highly unlikely that all of the infall is in the groups we have identified, as opposed

to infalling smaller groups we cannot discriminate and individual galaxies. To estimate what fraction this is of the infalling population, it would be necessary to separate the remaining population into an infalling population and those galaxies which have been through the cluster and are part of the virialized system.

It is, of course impossible to tag galaxies as members of one population or the other, but we can get a rough idea by dividing the cluster sample into members of the infalling groups and the remaining cluster/supercluster population and comparing their dynamical properties. The division of the non-group population into (1) infalling galaxies in smaller groups or singles on essentially radial orbits and (2) those that have already been through the cluster and have had their orbits isotropized to some extent, should manifest in a plot of redshifts relative to the cluster mean as a function of radius. Figure 11 shows that the “not in infalling groups” galaxies do indeed seem to show a declining velocity dispersion with increasing clusto-centric radius: in steps of 0.04-deg, 817, 731, 660, 562, and 591 km s<sup>-1</sup> (where we have excluded the halo of objects with  $|\Delta z| > 0.01$  that are either high-velocity infall or non-bound interlopers). An isotropic distribution would be near constant with radius, so this drop of  $\sim 40\%$  is indicative of a distribution containing a significant number of galaxies on radial (infalling) orbits. However, Dressler (1986) found a decline about twice-as-steep for HI-gas-deficient spirals in clusters that are thought to have been on highly radial orbits (see that paper’s Figure 4), so the result here suggests a mix of galaxies on radial orbits, both presumably infalling galaxies and galaxies that have made one or more passages through the cluster.

Taking a reasonable guess that the split between infalling and virialized as 50/50 (which covers the range 30/70 to 70/30) we conclude the infalling population at this epoch consists of roughly equal numbers of group and non-group galaxies. Not all of these “non-group” galaxies are single, isolated galaxies: many may in fact be members of infalling groups that are projected along the line of sight closer to the cluster center ( $R < 2$  Mpc), and are certainly members of poor groups with three or four members that are hard to isolate (but systems that may be massive enough to support some kind of preprocessing). Regardless, this rough estimate is sufficient to conclude that, in addition to 257 galaxies in infalling groups, there could be a similar number of galaxies that are not in the groups we have identified but are nevertheless infalling. The total infalling population would be, by this reasoning, roughly twice that of the remaining cluster population.

Thus, while there is a range of growth represented in these clusters, an increase by a factor of two by the present epoch seems a conservative estimate; at least half of this is in substantial ( $N > 5$  members) groups. Even without an accounting of the groups that might be infalling from the  $R \sim 5 - 10$ , Mpc, it is reasonable to conclude that this is the major epoch of growth for these systems.

During this period, from our observations of four ICBS clusters, the fraction of infalling galaxies that are in groups where preprocessing might occur is substantial, of order 50% or greater. This appears to be consistent with the predictions by McGee et al. and De Lucia et

al. but inconsistent with the prediction by Berrier et al.,. Again, quantifying the degree of agreement or contradiction requires a reasonable correspondence to be drawn between the ICBS cluster groups — dynamically cold, discrete groups of about 5-25 L\* galaxies — with the dark halo groups identified in the simulations. Regardless of the outcome of this comparison, the ICBS results are by themselves unambiguous: many, perhaps most galaxies are members of groups where some sort of “preprocessing” of star forming galaxies into passive galaxies could occur, long before these galaxies enter the more extreme cluster environment.

#### 4.3. Evidence for preprocessing from the spectral types of group galaxies

The PAS galaxies, which are non-starforming at the level  $sSFR < 10^{-11}$  yr<sup>-1</sup>, and the PSB (poststarburst) galaxies that will either to join or return to the PAS population, are systems where star formation has been effectively ended, either by internal processes or external agency. With our sample of groups in clusters and the field we can look to see if the PAS+PSB fraction is correlated with any properties of the groups themselves. We exclude six groups for this exercise, three cluster groups with  $N < 5$  members (too small for a statistical result) and three field groups with  $\tau_{enc} > 12$  Gyr (described below).

In Figure 12 we show distributions of some basic properties for cluster groups and field groups and filaments. The number distribution of group members is essentially the same for these two samples (see Tables 2, 3, and 4), but a more useful parameter is  $N_{tot}$ , a “complete” number of galaxies determined by fitting a Schechter (1976) function to bring all the groups (sampled at different redshifts and luminosities) to the same richness scale. Figure 12-a shows the distributions over  $N_{tot}$ , and Figure 12-c shows  $L_{gal}$ , a total luminosity in units of L\* calculated from a fit and extrapolation of the Schechter function for the group.

$L_{gal}$  is a luminosity, but it approximately scales to total mass within a factor of 20-30% that depends on the mix of starforming and passive galaxies with their range of mass-to-light ratios. The distributions over  $N_{tot}$ , and over  $L_{gal}$ , are indistinguishable for the cluster and field groups, as is the distribution of velocity dispersion  $\sigma$  (not shown). However, the distribution of sizes,  $R_{pair}$  (the mean of all pair separations), is clearly different for the two samples (Figure 12-b). The field distribution overlaps the cluster distribution but includes much larger systems. This may be a selection effect in that groups  $R_{pair} > 2$  Mpc are more difficult to pick out in fields dominated by a rich cluster, or it may be that such large, loose groups have been dispersed or their formation suppressed in the supercluster environment (which has had a higher density ‘plateau’ over cosmic time than the general field).

We also calculate  $\tau_{enc}$ , a typical time for a group member, moving at the speed of the velocity dispersion, to encounter another galaxy (within a fairly large impact parameter,  $R \sim 0.5$  Mpc). Since the encounter time  $\tau_{enc}$  depends linearly on the groups size, there are some field groups with significantly longer times than those of the cluster groups, all of which have  $\tau_{enc} \lesssim 3$  Gyr. A few of the field groups have  $\tau_{enc} > \tau_{Hubble}$ , long enough to



doubt the reality of the group as a physical association.

In Figure 13 we show the correlations of these various properties with the PAS+PSB fraction. There is no significant correlation of PAS+PSB with the group size (Figure 13-a), or, perhaps more surprisingly, with velocity dispersion  $\sigma$ , or  $\tau_{enc}$  (Figure 13-b). However, a weak correlation is found with a combination of size and velocity dispersion, the product  $R_{pair} \times \sigma^2$ , that is a measure of dynamical mass, although probably an unreliable one for groups like these that are unlikely to be well relaxed. Compared to this, Figure 13-d shows the improved correlation of the PAS+PSB fraction with the simple number of galaxies in the sample,  $N$ , and an even better correlation with  $N_{tot}$ , which is the number corrected via a Schechter function for sampling depth, (Figure 13-e).

The best correlation — a relatively good one — and is found with the total luminosity  $L_{gal}$  of the group. (Several significant outliers are discussed in the following section.) As explained above, a correlation of PAS+PSB versus  $L_{gal}$  is essentially one with group mass, estimated in the way that is most reliable for data such as these (compared to the less-secure dynamical mass). While it is not obvious why total group mass should be the independent variable best correlated with the PAS+PSB fraction, it clearly seems to be the case for the ICBS sample, so we will investigate this correlation and its implications in the next section, for the group sample and the larger and smaller mass scales also covered by our ICBS data.

#### 4.4. Growth of the passive population with structure scale

In Figure 14 we explore the correlation of the PAS+PSB fraction, those galaxies in which star formation has essentially ended, with the scale-size of the structure. For the groups infalling into four of the ICBS clusters, and the comparable field groups we have identified, group mass seems to be surprisingly well correlated with the PAS+PSB fraction, while  $\tau_{enc}$ , which tells us something about the galaxy-galaxy interaction rate, does not. A possible explanation for this is that the building of larger and larger structures through merging in hierarchical clustering is a series of events in which the passive fraction grows, rather than a steady transformation from star-forming to non-starforming galaxies as these stable groups age. This topic is explored further below.

Poggianti et al. (2006, see Fig. 10) have explored a similar relation in the fraction of starforming galaxies, the inverse of what we plot here, as a function of the velocity dispersion. For clusters,  $\sigma > 500 \text{ km s}^{-1}$ , a relation between velocity dispersion and the fraction of [O II]-emitting galaxies is found, in the sense that this fraction is bounded at progressively higher values as  $\sigma$  decreases. There is some evidence that this trend continues for poor clusters and groups,  $\sigma < 500 \text{ km s}^{-1}$ , the range covered by the ICBS groups. However, the dominant feature of this low- $\sigma$  part of the diagram is the wide scatter in the starforming fraction, with values ranging from 0% to 100%, with a median of about 50%. With such scatter and only 10 groups, it is hard to demonstrate a correlation of starforming fraction to velocity dispersion in this range. This is at least consistent with the lack of correlation for the ICBS groups between the non-starforming fraction and the velocity dispersion, but it is perhaps in-

teresting that the ICBS sample does not have such a wide scatter: 37 out of 42 values range in starforming fraction 70-100%, and the median value is 80%. Given the small Poggianti et al. sample for  $\sigma < 500 \text{ km s}^{-1}$ , these differences may not be statistically significant. Even so, the lack of a trend in the ICBS data for these groups suggests that  $\sigma$  is a less reliable indicator of “scale” for poorer, less dynamically mature systems compared to the  $\sigma > 500 \text{ km s}^{-1}$  clusters. It is for this reason that we think simply counting up the total luminosity or mass in galaxies is the best way to look for a correlation with group/cluster scale, and it would be interesting to recast the Poggianti et al. plot in that way.

A notable discrepancy with earlier work is the passive fraction of the ICBS cluster and field groups compared to the results of Balogh et al. (2009), who have investigated star formation in field groups culled from the CNOC study (Carlberg et al. 2001). The sample covers the redshift range  $0.25 < z < 0.55$  and is probably the most comparable in basic parameters to the ICBS groups. While the passive fraction in the ICBS groups — both cluster and field — cover the range 10–30% (except for two very populous groups that reach  $\sim 45\%$ , the Balogh et al. field groups run from 40–60% — the passive fraction in the Balogh et al. field is approaching that of the CNOC clusters. We see no easy way to reconcile this difference: the Balogh et al. groups are systematically more massive systems, from the mean velocity dispersion of  $\sim 350 \text{ km s}^{-1}$  compared to the ICBS mean of  $\sim 200 \text{ km s}^{-1}$  for the field groups, suggesting as much as a factor of three in mass. However, an extrapolation of the trend in Figure 14 by this amount (from a typical  $L_{gal}$  of 10 for the ICBS field groups to an estimated value of 30 for the CNOC groups, predicts a passive fraction of 30–40%, still significantly below the Balogh et al. passive fraction of 40–60%. Data quality influences the passive fraction only in the sense that low rates of star formation will be missed in lower S/N data: the ICBS measures of star formation are varied and robust; only high passive fractions are suspect with respect to data quality. We cannot at this time account for this significant difference in the passive fraction of the ICBS groups compared to the CNOC groups studied by Balogh, but we proceed with the confidence that the ICBS spectral types are consistent across the range of environments and mass covered by our study, so the relative differences we now discuss must be secure.

As discussed above, both the cluster and field groups of ICBS do in fact show a good correlation of PAS+PSB with the total luminosity or mass. The cluster groups, field groups, and the subset of field groups that are filamentary, are coded red, blue, and green, respectively, in Figure 14. We include error bars added for the PAS+PSB fraction that suggest that this correlation is as good as it could be given the errors. (The Poisson errors we use are overestimated somewhat due to the  $\sim 30\%$  incompleteness of the spectral catalog, that is, a larger number of group numbers are controlling the counting statistics.) The statistical errors are large for groups of this size, which typically contain only a less than a handful of PAS+PSB galaxies, nevertheless, it is interesting that the increasing fraction with  $L_{gal}$  appears in all three samples. This is remarkable, given the different environments of superclusters and the field, and

the clearly different structure of filaments. If verified by other, independent samples, this correlation suggests a process that is truly generic.

To further explore the dependence of PAS+PSB on  $L_{gal}$  we extend the sample to smaller and larger systems. The field galaxies that are not members of the groups and filaments of Tables 3 & 4 have been subdivided into galaxies that are isolated to the depth of our sample (roughly  $M^* + 2$ ), and those that were found using a friends-of-friends algorithm (see Paper 2) and had  $N < 5$  members. Most of the latter are relatively compact pairs and triplets, so we have assigned for purposes of display  $L_{gal} \approx 1.0$  for the isolated galaxies and  $L_{gal} \approx 2.0$  for the  $N < 5$  field groups. For both these samples there seems to be a floor of the PAS+PSB of  $\sim 10\%$ . This is consistent with the lowest  $L_{gal}$  groups in the  $N \geq 5$  sample. These scatter around 10%: the small groups that contain no PAS+PSB galaxies are merely statistical fluctuations on a small sample. In other words, there is a base level of about  $\sim 10\%$  PAS+PSB galaxies that is found for small groups and isolated galaxies. It is reasonable to speculate that these have been in place for a relatively long time, since  $z > 1$ , and that, as is well known for massive galaxies, averaged-sized galaxies can also reach a terminal state of star formation, either from very early processes that are properly thought of as early galaxy assembly,  $z > 2$ , or through later mergers  $1 < z < 2$ .

We note that the PAS+PSB fraction of the  $N < 5$  groups appears to be noticeably higher,  $\sim 20\%$ , from that of the isolated galaxies, and more comparable to the average of the richer groups. However, by selection, this sample contains a high fraction of binaries and compact groups that might be expected to have reached the higher PAS+PSB fraction found in the typical group.

At the other end of the  $L_{gal}$  scale in Figure 14, we use the full cluster/supercluster sample of each field, with the cluster groups omitted. As we have discussed above, these “non-group” galaxies are likely to be roughly divided between infalling galaxies that are isolated or in smaller groups, and galaxies that have passed through the virialized cluster population at least once. Taking the whole “non-group” population, we find that the five ICBS clusters (the solid symbols) lie, within the statistical errors, on an extrapolation of the trend of PAS+PSB vs.  $\log L_{gal}$  relation defined by the cluster groups. Perhaps more surprising is the placement of the richest infalling cluster group and the richest field group, each of which also falls along the extrapolation of the trend for the typical groups, and lie among the factor-of-two more massive clusters. These two have very different structures (see Figure 15): the cluster group SDSS1500B-2 is as concentrated as the cores of the 5 ICBS clusters; the field group RCS1102-10 is spread over the entire field and may in fact continue to the southeast (lower left). While the PAS and PSB galaxies in SDSS1500B-2 are, of course, limited to high-density environments, they are also found in similar abundance in the full range of environments of RCS1102-10, from high-density knots to medium-density groups to isolated galaxies.

#### 4.5. Cluster building, preprocessing, and implications for the “quenching” of star formation in galaxies

Our results concerning infall into the ICBS clusters show that this is an epoch of substantial growth in the history of massive clusters at  $z \sim 0.5$ . By not targeting only strong X-ray emitting clusters, or optically selecting the richest intermediate-redshift clusters, the ICBS shows how more typical rich clusters grew during this epoch. For RCS0221A, RCS1102B, SDSS1500A, and SDSS1500B, we find and easily identifiable infall of groups comprised of 257 galaxies, as well as the expectation of infall for a sizable fraction of the remaining 786 cluster galaxies in these four fields.

“Quenching” is a popular shorthand for a process capable of ending star formation in starforming galaxies. As described by Peng et al. (2010), quenching refers to one or more physical processes, driven internally (e.g., secular evolution and starbursts *within* a galaxy) or externally (e.g., mergers or ram-pressure stripping). These authors distinguish this from the general decline in the specific star formation rate of starforming galaxies since  $z \sim 2$ , possibly the result of a decline in available gas that is capable of sustaining star formation. This separation may not be a clean one, however, since the decline in available gas may itself be a function of environment: many of today’s passive galaxies, especially massive ones, may have ceased star formation at very early times because they efficiently processed the accessible gas into stars.

Our results here suggest that some  $\sim 10\%$  of galaxies, even in the lowest density environments had already ceased significant star formation by  $z \sim 1$ . Presumably this could be a mix of early mergers of individual galaxies, fossil groups, or the occasional massive galaxy that underwent efficient star formation at  $z \sim 2$  and exhausted the local gas supply. Higher redshift measurements of this “base level,” as well as studies of mass and luminosity functions, and morphology over cosmic time, might be able to discriminate which paths lead these galaxies to a permanently passive state.

From this base level, we see a clear signature of increasing fraction of passive galaxies once the mass scale of a group rises above  $5L^*$ , or  $5M^*$ . This increasing fraction is usually associated with higher density environments, but some passive galaxies are also found in relatively low-density parts of these moderate-sized groups. A prevalent idea that has come from the  $\Lambda$ CDM simulations is that passive galaxies are satellites whose halos have been incorporated into more massive “central” galaxies, as discussed in van den Bosch et al. (2008, see also Weinmann et al. 2010). In this connection, we show in Figure 16 the distribution of passive galaxies in the ICBS cluster groups. Although our data are only  $\sim 70\%$  complete, there seems to be a wide distribution of environments — and no clear companions — for a majority of the passive systems in our study. While apparently inconsistent with the notion that passive galaxies are mostly likely to be satellite galaxies, van den Bosch et al. show in their study of a large SDSS sample that this phenomenon is a strong function of mass, declining from the dominant fraction ( $\sim 70\%$ ) of the population for galaxies with stellar masses of  $\sim 2 \times 10^9 M_\odot$  to virtually nil at  $\sim 2 \times 10^{11} M_\odot$ . The majority of our sample are galaxies intermediate between these two limits, so perhaps a sizable minority of galaxies that ceased star formation when they were

incorporated into central galaxies is after all consistent with what we find in the ICBS group sample.

The trend of gradually rising PAS+PSB fraction with increasing group mass might be explained by the effects of mergers (roughly equal mass systems) and accretions (higher mass ratios), or the increasing loss of gas supply (starvation), all processes that should be favored in more populous systems. However, our data would seem to argue against any steady “cooking” process that operates over the lifetime of the group, by the lack of any correlation with  $\tau_{enc}$  (see Figure 13-b). The objection might be overcome, however, by recognizing that, in a hierarchical model of structure growth, such systems are built from the mergers of smaller groups. If we regard the coalescence of groups themselves as the event that bumps up the number of passive galaxies through one or more of the “interaction” processes, the lack of a correlation with  $\tau_{enc}$ , and the correlation with group mass, is readily explained. We discuss other evidence bearing on this model in §4.7 and §4.8.

Projecting the relationship to the higher masses of the clusters, we see in Figure 14 a track that could well be populated with increasingly rich groups not in our sample, reaching the  $\sim 50\%$  fraction of PAS+PSB galaxies in these more massive systems. Indeed, the two rich groups that are in our sample seem to confirm the idea that this modest process that we identify with interactions in the group environment is capable of building the high level of non-starforming galaxies. On the other hand, our sample presents what appears to be prima facie evidence for a cluster specific process: the 60-80% fractions of PAS+PSB galaxies in the four groups that are centrally located (marked with a red ‘X’ in Figure 14). Whether these are groups or filaments, the projection of these four cold substructures right on the highest density regions of the clusters leaves little doubt that they are passing through, or have passed through, the cluster center. The exceptionally high PAS+PSB fraction points to a cluster-core-specific mechanism — for example, ram-pressure stripping — that is far more rapid and efficacious than any preprocessing that is happening in the other cluster and field groups. We might wonder, then, if we have obscured such an effect by adding the dense cluster environment to the outer halo of galaxies, which includes single and small-group infall — there could be a more dramatic trend in Figure 14 attributable to a more effective or unique process coming into play when a higher mass scale or unique environment is encountered.

To explore this possibility, we have partitioned the full sample of each cluster, with the infall of groups subtracted, into a “core” and “halo” population, divided at  $r_{200}$ , the virial radius (Table 1). The “cluster core” points Figure 14 do in fact show a 50-80% PAS+PSB fraction — they lie far enough above the trend established by the groups to argue for one or more cluster specific processes.

What about the cluster halos, which seem to be off in a kind of ‘no-man’s land’ in Figure 14? They are not the single systems of the cluster cores, which can be parameterized by an  $L_{gal}$  and a PAS+PSB fraction, because (1) the appropriate mass to use for members of this population is that of a single galaxy or a poor group, and (2) they are almost certainly a mix of infalling galaxies and galaxies that have been through the cluster core region at

least once. As we argued above, it is reasonable from the run of velocity dispersion with clusto-centric radius (Figure 11) to regard this as an approximately equal mix of infalling and “through the core” galaxies, with different PAS+PSB fractions expected for each. For the infalling population, moving them to the appropriate  $L_{gal}$  for singles and poor groups, we expect a PAS+PSB fraction on the order of 15%, a population that is largely “unprocessed.” For the “through the core” population we take the cluster-core fraction of 60% PAS+PSB. Adding these together in a roughly 50/50 mix would predict a  $\sim 37\%$  PAS+PSB fraction, compared to the weighted average for these cluster halos, 135 PAS+PSB galaxies out of a total of 429 = 31%. This rough agreement could be improved by raising the infall fraction to 60-70%, but this is beyond the level of argument. The point is that a mix of infalling galaxies, with an “unprocessed” fraction determined from another sample, and a “processed” fraction determined from yet another sample, accounts reasonably well for the PAS+PSB fraction we measure for this halo population outside the virial radius.

#### 4.6. Do starbursts play a major role in the production of PAS galaxies?

In this section we address the question of the numerous starburst galaxies we have identified in the ICBS program — both active and post-starburst. As described in Paper I, we have adopted specific criteria for identifying these from H $\delta$  and [O II] emission that have been validated with well-studied present-epoch samples. For the ICBS sample  $0.31 < z < 0.54$  we find a level of  $20\% \pm 10\%$  for all starbursts (SBH+SBO+PSB) in every environment studied in the ICBS, from isolated field, to groups, to rich clusters. These specific criteria are important, for our definition of active “starbursts” extends down to galaxies where the SFR at the epoch of observation is only  $\sim 3$  times that of the past average. The lower end of the range selected with our criteria includes systems with a much more moderate starburst than even the lower luminosity *LIRG* galaxies that have been discovered in infrared surveys. As with the passive galaxies, the post-starburst category requires a uniform and well-defined boundary between starforming and non-starforming systems.

Concerning poststarbursts in particular, we have presented evidence for the ubiquity of the minority but potentially important population at intermediate-redshift in a series of papers (see, e.g., Dressler & Gunn 1983; Oemler et al. 1997; Dressler et al. 1999; Poggianti et al. 1999) as have other studies (e.g. Couch & Sharples 1987; Barger et al. 1996; Tran et al. 2003; Lemaux et al. 2010). Poggianti et al. 2009 have in particular conducted an extensive study of poststarbursts over a wide range of environments at  $z = 0.4 - 0.8$ . Nevertheless, some other studies have either questioned the prevalence of such a population (see Balogh et al. 1999 – cf Dressler et al. 2004; Kelson et al. 2001) or de-emphasized its importance (e.g., van Dokkum et al. 2000; Ellingson et al. 2001). Key to the doubt expressed about the importance of the starburst is the suggestion that the poststarburst signature is really nothing more than the sharp truncation of star formation in a very active galaxy, without a burst.

A abrupt end ( $\tau \lesssim 200$  Myr) of star formation in a

galaxy whose current SFR is close to its past average will indeed develop a spectrum that is hard to distinguish from a *mild* starburst. However, in modeling this affect, Poggianti et al. (1999, see also Poggianti 2004) concluded that  $H\delta \approx 5 \text{ \AA}$  is a limit reached by truncating such a system (in particular, for an intermediate-redshift galaxy that has been forming stars with a normal initial-mass-function and constant SFR since  $z \gtrsim 2$ ). Poggianti et al. noted that approximately one-third of the galaxies identified as PSB in the *Morphs* sample exceed this limit. We find the same fraction in the PSB sample of the ICBS:  $19/55 = 35\%$ . Taking into account the decline in  $H\delta$  strength that these systems *must* experience as they age, over a longer time scale, this accounts for about another third of the observed sample, leaving at most one-third to be identified as simply truncated systems with  $3 \text{ \AA} < H\delta < 5 \text{ \AA}$ .

The one-third fraction should moreover be an upper limit because most SFRs decline with cosmic time. However, a new determination of the histories of star formation in the ICBS galaxies by Oemler et al. (2012b – Paper 2, see also Gladders et al. 2012) suggests that a small but non-negligible fraction of galaxies are genuinely younger, in the sense of SFRs that have peaked more recently than  $z \sim 2$ . In a future paper we will use a representative distribution of star formation histories to refine this estimate of the fraction of poststarburst galaxies with  $H\delta > 3 \text{ \AA}$  that could be the result of simple truncation of star formation, with no prior burst required.

These considerations do not, however, affect the general conclusion that the majority of the PSBs are in fact poststarbursts. The abundance of SBH + SBO galaxies in the ICBS sample, which are unambiguous cases of mild-to-moderate *active* starbursts, strongly supports the conclusion that a sizable fraction of the PSB sample must come from starbursts rather than truncation. From the Spitzer observations of two of the ICBS fields, we concluded that even some of the PSB are active starbursts, probably nuclear bursts that are more easily buried by dust.

For the purposes of this discussion, then, we take as a given that active starbursts and poststarbursts are a significant component of the intermediate-redshift galaxy population, and turn our attention to how the SBH+SBO and PSB galaxies relate to the ordinary CSF and PAS galaxies.

In Figure 14 we showed the fraction of PAS+PSB galaxies over the full range of galaxy environments. Assuming that the PSB galaxies are unlikely to regain future SFRs of even a few tenths of a solar-mass per year, the PAS+PSB are the complete population of galaxies with masses  $M \gtrsim 10^{10} M_{\odot}$  that have been “quenched,” by whatever internal or external means. If we instead consider the fractions of PAS and PSB galaxies separately, over the full range of environments, we can apply a simple timescale argument to investigate whether starbursts play a significant role in increasing the PAS population. Figure 17-a shows the fraction of PAS and PSB galaxies separately over the full range of environments sampled in the ICBS. The samples are much the same as in Figure 14, but we have combined the results for the different fields for the isolated galaxies, small groups, cluster cores, binned the cluster and field groups (including filaments),

and omitted the composite populations of clusters embedded in their superclusters (which are mixed rather than unique environments). The points with (Poisson) error bars are (1) four-field averages of isolated galaxies and the small groups, placed at  $L_{gal} = 1.0$  &  $2.0$ , respectively, and at increasingly larger  $L_{gal}$  (2) averages of cluster groups, field groups and field filaments, in bins in which the summed  $L_{gal}$  is  $\sim 80 L^*$  (containing between 94 and 129 galaxies per bin). The stars representing the combined 5 ICBS cluster cores ( $R < 0.5$  Mpc) have error bars that are smaller than the symbol, and their placement along the  $L_{gal}$  axis is approximate.

In addition to the unsurprising result of the steady increase in the PAS fraction of intermediate-redshift galaxies, from  $\sim 10\%$  for the isolated field galaxies to  $\sim 70\%$  for the cores of rich clusters, Figure 17-a shows a remarkable result: the PSB track the PAS fraction in the sense that the PSB fraction is  $\sim 10\%$  of the PAS fraction *in all environments*.

A comparison of the fraction of active starbursts, SBH+SBO, to the fraction of continuously star forming galaxies, CSF, shown in Figure 17-b, exhibits a similar effect. Compared to the PAS fraction, the CSF fraction declines steadily over the  $L_{gal}$  range, from a population that dominates PAS galaxies by many-to-one in the field, to  $\sim 1:1$  in rich groups and clusters, dropping to only  $1:5$  of the PAS in the cluster cores. (Even this small remaining CSF population is likely exaggerated, since some CSF types are only projections along the line-of-sight to the cluster core.) Like the PSB and PAS fractions, the active starbursts (SBH+SBO) track the CSF population, in this case displaced by a factor of 4, that is, it is approximately 4 times less populous than the CSF sample *in all environments*. The fraction of active starbursts matches or exceeds the fraction of PAS galaxies for isolated galaxies and the small group environment, and in the cluster cores the fraction of active starbursts decline to the same  $\sim 10\%$  that the PSB risen to.

Two basic conclusions can be drawn from Figure 17. First, active starbursts, in environments running from the isolated field galaxies to modest-sized groups, cannot be a path to passive (PAS) galaxies — there are far too many of them. The lifetime of these bursts is likely to be no more than 1 Gyr — indeed, this is long for a starburst.<sup>6</sup> In environments like the field and small-to-moderate groups, the (SBH+SBO)/PAS ratio is about 1:1. If most of SBH+SBO turned to PAS galaxies, the fraction of these would double in a Gyr or less. It would seem that most of the SBH and SBO galaxies in these environments must return to the pre-starburst CSF state in such environments, as was also concluded by Poggianti et al. (1999). We note, however, that this conclusion weakens considerably for richer groups and cluster populations. For these environments, SBH+SBO fraction falls to  $\sim 10\%$  while the PAS fraction has risen to 40% or more, and, again for these environments, modest growth in the PAS fraction from  $z \sim 0.5$  to the present-epoch is observed (Li et al. 2009; 2012). So, when combined with the fact that the active starburst population is declining

<sup>6</sup> We have, however, argued in Oemler et al. (2009) that the degree to which A stars dominate the light necessitates a minimum lifetime  $\tau > 200$  Myr, the lifetime an early A star, and sufficient time for such a stars to migrate from the dusty sites of their birth.

from  $z \sim 0.5$  to the present *in all environments* (Dressler et al. 2009a), it appears that active starbursts could be significant contributors to the PAS population of denser intermediate-redshift environments.

While most active starbursts — members of the field population — cannot be linked one-to-one with the quenching of starforming galaxies to form PAS galaxies, the situation more favorable for PSB galaxies. Indeed, a PSB/PAS fraction of  $\sim 10\%$  in all environments — very different from the varying (SBH+SBO)/PAS fraction across environments) in fact urges a direct connection of the PSB phase to a quenching event that produces a new PAS galaxy. The decay time for this phase,  $\tau \lesssim 500$  Myr (more certain in this case because the absence of starformation constrains the spectral evolution), suggests that — if the PSB fraction remained constant from  $z \sim 0.5$  to the present — the PAS fraction would approximately double. However, there is good evidence for a steep decline in the fraction of PSBs in the field, from the ICBS value of  $\sim 1\%$  to a level of  $\sim 0.1\%$  at the present epoch (Zabludoff et al. 1996; Wild et al. 2009), so it would appear that decaying PSBs would not overproduce PAS galaxies, even with the slow growth of the passive galaxy population in the field since  $z \sim 0.5$  found by, e.g., Faber et al. (2007) and Brown et al. (2007). The situation is much the same for rich groups and clusters: the same 10:1 ratio of PAS/PSB is found, and the poststarburst fraction is known to decline substantially with time (the PSB class was essentially unknown until intermediate-redshift clusters were studied). The problem, however, is that extrapolating back in time to  $z \sim 1$  in both the field and in clusters similar fractions of PSB galaxies are found, for example, in the extensive study of the CL1604 supercluster (Lemaux et al. 2010), a poststarburst fraction of  $\sim 10\text{--}15\%$  is found in the lower density environments outside the virialized clusters (B.C. Lemaux, private communication; see also EDisCS references). Therefore, while the overproduction of PAS galaxies by the decay of PSB galaxies since  $z \sim 0.5$  would not be a problem, it would likely be a serious problem for the earlier epoch  $z \sim 1$  to  $z \sim 0.5$ .

In this conclusion, that the PSB galaxies cannot be the dominant mechanism for producing the PAS population between  $z \sim 0.5$  and the present, we are in agreement with De Lucia et al. (2009), whose argument includes the issue of generally lower luminosity (mass) of PSB compared to PAS galaxies, which is illustrated by the ICBS sample Figure 1-c (-a). The small sample in De Lucia et al. is an issue — the two clusters in their study show very different PSB/PAS fractions, undoubtedly due to the short time scales of the PSB phenomenon and resultant statistical uncertainties. Wild et al. (2009) come to a conclusion that could also be consistent with the ICBS result, finding a possible production of  $\sim 40\%$  of PAS galaxies in another small sample at  $z = 0.5 - 1.0$ .

In summary, while it is likely that some fraction of starbursts and poststarbursts are phases on the path to passive galaxies, a model in which this is the dominant path is troubled by the short timescale of the phenomena and the commonness of these types, when compared to the relatively slowly changing populations of passive galaxies — a point made by De Lucia et al. (2011) for quenching mechanisms in general. The fact that the starburst phenomenon is in rapid decline since  $z = 0.5$  helps, but

observations of galaxies at higher redshift,  $0.6 < z < 1.0$  show only a small change of the starburst fraction, so overproduction during this earlier time is likely to be a serious problem. Furthermore, there are clearly important trends that do not seem to flow easily from such a model: the field population of PAS galaxies changes very slowly to the current epoch while the fraction of PAS in rich groups and clusters grows substantially, suggesting an environmentally sensitive quenching method, while the PSB/PAS fraction is near-constant from the field to rich clusters at  $z \sim 0.5$  and rapidly declining for all environments to the present day. Likewise, (SBH+SBO)/CSF is constant over all environments, but the timescale argument indicates that only in rich groups and clusters could these be major contributors to the PAS population, and only a very small fraction can be funneled to PAS galaxies in the lower-density field. As both McGee et al. (2009) and De Lucia et al. have suggested, the mild trends of PAS growth point to quenching mechanisms with long time scales,  $\tau > 2$  Gyr, and these are not compatible with the starburst signature. A significant fraction of PAS galaxies could be the result of starbursts, but it appears that most cannot.

#### 4.7. A Different Picture: starbursts are a signature of mergers across all environments

If starburst and poststarburst galaxies are too numerous to be phases in the quenching of starforming galaxies to produce passive galaxies, then perhaps there is a better explanation. Rather than a phase of PAS production, what if the starbursts are events in which the PAS and CSF galaxies are ‘targets’? The approximately constant ratios of 1:10 for PSB/PAS and 1:4 for (SBH+SBO)/CSF over all environments suggests an alternative picture, one in which active starbursts, and poststarbursts, are the result of minor mergers and accretions of gas-rich satellites onto PAS and CSF galaxies, respectively. That is, when a CSF galaxy suffers a minor merger or accretes a satellite, its SFR can increase significantly, resulting in an SBO or (dust-obscured) SBH and later returning to the CSF population. A PAS galaxy accreting a gas rich companion would result in a spectrum like that of an early type spiral, before returning to the PAS spectral class. The fact that a starburst has occurred would be difficult to distinguish if the continuum light is dominated by an old stellar population. The ICBS sample does in fact include red galaxies with high SFRs; this can be deduced from Figure 18, which shows that — in addition to an excellent correlation of specific star formation rate with rest-frame B-V color, there are galaxies with very red colors (old stellar populations) with very high star formation rates. Some of these could be the progenitors of PSBs in this model, active starbursts that cannot be identified as such because our criteria for active starbursts — anomalously strong H $\delta$  or [O II] — is compromised by a strong continuum light from old stars.

The attraction of this model is that it explains the ICBS observations as well as results of numerous other studies. The starburst phenomenon is pervasive among high redshift galaxies, especially when considering the relatively short duty cycle, but the connection of this to popular mechanisms such as ram-pressure stripping or strangulation is forced, to say the least. These mechanisms are expected to act on a longer timescale — an

attractive feature when trying to account for quenching of starforming galaxies and the growth of the PAS population, but ill-matched to the starburst signature. In contrast, mergers undoubtedly play a significant role in the evolution of many galaxies, and their connection to the starburst phenomenon — first elucidated by Zabludoff et al. (1996) in their study of poststarbursts in the low-redshift, field-dominated Las Campanas Redshift Survey — has also cropped up in morphological studies of active starbursts and poststarbursts in rich clusters (see Oemler 1999, §6). Mergers are known to lead to rapidly increasing and decreasing star formation rates, for which the spectral types SBH, SBO, and PSB are easily associated. Furthermore, by operating in a wide range in environments, minor mergers and accretions provide a natural explanation to the ubiquity of these starburst phenomenon in field, groups, and clusters, as well as contributing in an expected way to the steep decline in this activity over the last  $\sim 5$  Gyr. While the focus has been on major mergers as a method of producing spheroidal stellar systems from disk systems, particularly at early times ( $z \gtrsim 2$ ), minor mergers and accretions are far more common events and offer the possibility of not drastically altering the basic properties of the primary galaxy. Thus, identifying the precursors of most active starbursts as normal starforming galaxies, and the precursor of poststarbursts with passive galaxies, explains the tracking of PSB to PAS and (SBH+SBO)/CSF seen in Figure 17 in a natural way.

#### 4.8. *The big picture?*

Is there a notional model that approximately describes the histories of star formation and structure evolution of galaxies with redshift and environment, and identifies the most influential processes? Despite great progress in the last few decades in quantifying the characteristics of galaxies over most of cosmic time, and the identification of many processes thought to influence galaxy evolution, it has been difficult to agree on a picture that explains the basic data. In this paper we have used observations of intermediate-redshift galaxies over the full range of environment, from isolated field galaxies to the cores of rich clusters. We have presented evidence that suggests that the “quenching process” that turns starforming galaxies into passive galaxies is for the most part the result of slow processes such as starvation that are particularly effective in galaxy groups. The other notable process at higher redshift — the increasing frequency of starbursts — is not, we argue contributing very much to this slow quenching activity, but instead is a signal of an increasing merger rate at higher redshifts. These starbursts may have a significant effect on galaxy structure/morphology, and a detailed understanding of the starburst phenomenon is of course necessary for a complete description of the star formation history of many if not most galaxies.

Starting with some speculation about the evolution of galaxies before  $z = 2$ , these two basic programs of starvation quenching and merging starbursts could frame a picture of galaxy evolution that accounts for much of what is observed. We take  $z \sim 2$  as the start time for our description, identifying the epoch  $2 < z < 6$  as the time of galaxy assembly, during which the component structures are not directly comparable to the galaxy types we see to-

day. Most galaxies are starforming, even today, though on-average their rates of star formation are plummeting since  $z \sim 1$ . However, it is clear that some fraction of passive galaxies formed the bulk of their stars early,  $z \gtrsim 2$ , and that this forms the basis for the  $\lesssim 10\%$  fraction of passive galaxies that are found in even the sparsest environments and as far back as  $z \sim 1.5$ . This does not necessarily mean that they remain undisturbed and free of star formation at later epochs, indeed, the “red nuggets” — small, relatively massive, passive galaxies at  $z \sim 2$  (see, e.g., van Dokkum et al. 2008; Williams et al. 2010) are thought to evolve to somewhat more massive but substantially larger spheroidal-dominated systems by the present day.

Today, elliptical and S0 galaxies are the morphologies associated with this base population of passive galaxies, and it is worth remembering that, because 95% of galaxies live outside of the rich cluster environment, these elliptical and S0 galaxies that are either isolated or in loose groups are the majority of the population of passive galaxies, even though they are more *frequent* in denser environments. As hierarchical clustering proceeds since  $z \sim 2$  major mergers add to the passive population, especially in the densest environments, but the merger rate is declining with time, and major mergers — two roughly equal masses — are the least common. These events, if involving gas rich galaxies, are the well-known LIRG and ULIRG galaxies, and “dry” mergers (PAS) when they are not. Here we have suggested that the much-more-numerous minor mergers and accretions, perturb and evolve the properties of the larger galaxies, events that result as mild-to-moderate starbursts, but in most cases leave the galaxy fundamentally unaltered.

However, another important result of the last decade is that the elliptical galaxy fraction is slowly changing since  $z \sim 1$  and maybe earlier (GDDS reference), while the numbers of S0 galaxies have increased rapidly even since  $z = 1$ . These are the passive galaxies that are produced in by quenching, through starvation or stripping, and it would seem that the main location of this transformation is in galaxy groups. The quenching mechanisms that *are* sensitive to environment are starvation (Larson et al. 1980; Bekki et al. 2002), ram pressure stripping (Gunn & Gott 1972; Balsara et al. 1994; Abadi et al. 1999; Quilis et al. 2001; Bekki et al. 2009), and harassment (Richstone 1976; Moore et al. 1998). We have argued here that the hierarchical merging of groups are events that initiate the quenching for more and more galaxies, as time progresses, and that such “preprocessing” is able to produce a majority of the passive systems that we dominate the rich clusters, well before these groups are incorporated into the clusters. However, there is room in this picture for cluster-specific processes like ram-pressure or tidal stripping that further quench starforming galaxies to reach the  $\sim 80\%$  fraction of passive galaxies found in the densest environments.

We believe the minor mergers and accretions that we believe are the main drivers of starbursts in galaxies at higher redshift. Although we have no morphological information from HST imaging to look for merging associated with the SBH, SBO, and PSB galaxies in the ICBS sample, there are abundant examples for the environment of the rich clusters of the Morphs study. Figure 8 of Dressler et al. (1999) shows minor mergers ( $M1/M2 =$

3:1 to 10:1) and perhaps even accretion events ( $M1/M2 > 10:1$ ) for more than half of the examples of e(a), e(b), and k+a or a+k, the categories that correspond to the SBH, SBO, and PSB of this study. Unlike the transformational processes that we have identified as increasing the passive population, mergers and accretions are not strongly affected by environment.

so in this ‘big picture’ they cannot be the major mechanism for building up the passive populations in denser environments that becomes evident around  $z = 1.5$  and important for  $z < 1$ .

Boselli et al. (2006) comprehensively review of the environmental mechanisms that can turn starforming galaxies into passive ones. ‘Starvation’ (or strangulation) is currently the most-cited mechanism for turning off star formation to produce passive galaxies (Larson et al. 1980; Bekki et al. 2002). This process is almost certainly too slow to result in even the weaker PSB spectral signature, the ones that do not require a burst (discussed above). However, this slower time scale,  $\tau \gtrsim 2$  Gyr, is a virtue in explaining the growth of the passive population, as explained in the previous section.

It is possible that ram-pressure stripping (Gunn & Gott 1972; Balsara et al. 1994; Abadi et al. 1999; Quilis et al. 2001; Bekki 2009) can result in a sufficiently sudden end to star formation to produce at least the minority of the PSB spectrum galaxies, those that require only truncation of star formation on a timescale  $\tau < 1$  Gyr. There is evidence, however, that although ram-pressure stripping is able to clear spiral disks of HI gas in central cluster regions, the fate of the denser molecular gas towards the galaxy’s center is less (Kenny & Young 1988; see also Boselli & Gavazzi (2006). If true, ram-pressure stripping should only curtail star formation on a longer time scale ( $\tau \gtrsim 10^9$  yr), the SFR declining relatively slowly as the disk gas is used up in astration. The theoretical modeling in these studies imply that the effects of starvation and ram-pressure stripping may both be effective at stopping star formation, but not abruptly, and unable to populate the PSB class.

However, recent work suggests that ram-pressure might do more than this. As first suggested by Dressler & Gunn (1983), the hydrodynamic interaction of a gas-rich disk with a hot, high-pressure intracluster medium (IGM) might trigger a burst of star formation in an infalling cluster galaxy. This idea has been explored recently (Kapferer et al. 2008, 2009) along with the idea that the static pressure alone of the iIGM could trigger a starburst in a gas rich disk galaxy (Bekki & Couch 2003; Bekki et al. 2010). There is at least one case where bursts of star formation induced by ram-pressure may have been observed (Cortese et al. 2006), and the effects appear to be dramatic. Of course, even if ram-pressure or a static high-pressure IGM can induce starbursts, this mechanism only functions over a small range of the environments studied here — in the cores of rich clusters. However, this is exactly where the fraction of starbursts is highest, so it could be that these are contributing to the passive population in this unique environment.

Moran et al. (2008), in studies of two intermediate-redshift clusters, find examples of “passive” spiral galaxies that they believe are transitioning from active spirals to S0 galaxies. They identify the agent as ram pressure stripping by showing that these objects are only found

in regions where the intercluster gas is of sufficient density. Their sample includes both objects undergoing a slow evolution (undetected in UV light), and those with more recent signs of star formation — detected in the UV, and possibly a burst.

Harassment, as developed by Moore et al. (1998), is a cluster-specific process in which a galaxy is whittled down by a combination of encounters with other galaxies and through the tidal field of the cluster as it traverses the cluster core. Moore et al. did in fact, suggest that harassment of a gas-rich galaxy could produce starbursts, in a manner similar to the possibility of ram-pressure induced star formation, but harassment is mostly effective for lower mass galaxies and, of course, only operates in dense environments, so it can only account for at most a small fraction of starburst galaxies.

We conclude, as others have, that strangulation and ram pressure stripping are likely the dominant mechanisms for turning star forming galaxies into passive ones. Because these are strongly dependent on environment, and operate more slowly than mergers, they are consistent with the basic fact that the passive fraction is growing mostly in denser environments since  $z < 1.5$ , and slowly. Mergers, on the other hand, and likely to be primarily responsible for the starburst phenomenon (with a possible contribution from ram-pressure stripping and harassment in cluster cores). Mergers — major and minor — can operate effectively over a wide range of environments — even in clusters. The two distinctive features of this model are (1) starbursts are not an important quenching mechanism, and (2) poststarburst galaxies are more common in dense environments not because they are produced by an environmentally sensitive mechanism, but because they are tied to the large population of passive galaxies in such environments. Both conclusions are at-odds with those of previous studies, including our own.

#### 4.9. *Mergers and environment, and the connection to S0 galaxies*

Major and minor mergers, and strong tidal interactions, are clearly viable in the lowest density environments, however, the group environment has long been touted as the environment where mergers and tidal encounters are most favored (Just et al. 2010 – need other references, especially early ones), because of a “sweet spot” of higher galaxy density and a moderate encounter speed, when compared rich clusters where galaxy densities are very high but encounter velocities are sufficiently high to discourage mergers. A recent study by Wilman et al. (2009) of groups at intermediate redshift,  $z \sim 0.4$  — the first to accomplish this difficult observation program, provides strong support for this notion, concluding:

We conclude that the group and subgroup environments must be dominant for the formation of S0 galaxies, and that minor mergers, galaxy harassment, and tidal interactions are the most likely responsible mechanisms.

Just et al. (2010, 2011) have also highlighted the role of subgroups as a preprocessing site, specifically in the production of S0 galaxies, which are frequently cited as

a common outcome of such encounters (Bekki & Couch 2011). Indeed, Bekki (1998, 2001) claimed that S0 galaxies would be likely result of mergers of unequal galaxies with masses in the ratio 3:1, which are the most common encounters. This is significant, because it is well established that the S0 population, and not the elliptical population, appears to grow rapidly over the epoch  $0 < z < 1$ , at least in clusters and groups (Dressler et al. 1997; Postman et al. 2005; Desai et al. 2007; Poggiant et al. 2008). \*\*\*Do we know anything about poor groups and the field?\*\*\*

With both field and groups identified as fertile ground for galaxy interaction and mergers, it seems that only rich clusters would be the only unfavorable locations, and this view, that high velocity dispersions would suppress the merger rate (old reference?) held sway for decades. However, as first pointed out by Mihos (2004), the building of clusters through in the context of hierarchical clustering changes the situation dramatically. Mihos suggested that even the cluster environment, in particular, the case of subgroups falling into rich clusters, a wide range of slow and fast tidal encounters, and even mergers, would occur at rates high enough to play a major role in galaxy evolution. In fact, Mihos was the first to use the term “preprocessing” (need to verify this! – I could find no earlier reference) in describing the role that mergers and interactions might play in the group phase of cluster evolution, and he predicted a range of starburst phenomena, from moderate and over the full galactic disk, to central and strong, that close encounters of group and cluster galaxies could produce.

In one of the clearest case of subgroups in a rich environment, Oemler et al. (2009) used *HST* images to investigate starburst and poststarburst galaxies in Abell 851, one of the clearest cases of merging substructure in the rich cluster environment. This study found a large population of such galaxies, some of them cases of hidden starbursts that could only be detected through their  $24\ \mu\text{m}$  emission. The latter were identified as the youngest systems, and mostly had disturbed morphologies, including tidal signatures of major mergers. Oemler et al. show that — throughout the cluster — disturbed morphologies (indicative of tidal encounters or mergers) are common, particularly for the youngest (most recent) starbursts, although some poststarburst galaxies appear quite normal compared to a present-epoch early-type spiral.

\*\*\*Note: We have good ground-based imaging of RCS1102 and are going to check on the morphologies of the galaxies with respect to the different spectral-type categories to see if there is anything there.\*\*\*

While these studies have sensibly identified the minor mergers and accretions as production mechanisms of S0 galaxies, the present study has added to the evidence to other studies that the primary mechanism for quenching star formation in spirals is likely to be strangulation or ram-pressure stripping, based on considerations of overproduction if most starbursts and poststarbursts are adding to the passive galaxy population. Perhaps the resolution of this problem is that the rich cluster environment is the only one where quenching through starbursts is at least possible by the numbers, but we believe that this is not the best resolution of this apparent contradiction. Rather, we believe that we must be careful to distinguish between the evolution of structure and

that of the stellar population. A combination of what these studies have found, and what we have proposed here, is that mechanisms like strangulation are responsible for the evolution of the stellar population, but that minor mergers and accretions that take place in the densest environments — that we observe as active starbursts and particularly poststarbursts — are growing the large bulges of S0 galaxies that are a distinctive feature of the class.

## 5. SUMMARY

Our spectroscopic and photometric study of 4 fields of  $\sim 0.5$  deg diameter has produced high quality data for some 2200 galaxies in 5 rich clusters and the field,  $0.31 < z < 0.54$ . From these data we have measured galaxy magnitudes, colors, line strengths, and velocities and computed galaxy star formation rates and masses. Using these basic data we have separated galaxies into 5 spectral types: passive, continuously star forming, two types of active starburst, and poststarburst.

For 4 of the 5 clusters in our sample, we find substantial infall of moderate-moderate cold-sized groups with typically 10-20 members; these groups contribute roughly half of the infall into the clusters, and the total infall within  $R < 5$  Mpc is sufficient to double the mass of the virialized cluster. The ICBS clusters are more representative of clusters at intermediate redshift than those selected by, for example, strong X-ray emission: the one rich, regular cluster of this type in the ICBS sample shows much less infall and is presumably in a more advanced dynamical state.

The groups infalling into the clusters have been compared to field groups and filaments of similar size, mass, and velocity dispersion. For all three samples we find a factor of 2-3 growth in the fraction of passive galaxies from the smallest to the largest groups, indicating that preprocessing in groups is substantial. However, there is also evidence that in rich cluster cores additional quenching mechanisms “kick in” and further elevating the passive fraction. Cluster groups that are projected along the cluster center, presumably infalling or exiting from the cluster core, show this effect strongly: their fraction of passive galaxies is  $\sim 70$ -80%.

Active and passive starbursts together make up  $\sim 20\%$  of the intermediate galaxy population, so common that — given the  $\tau < 500$  Myr the timescale of the starburst phenomenon — it is unlikely that they are indicative of a quenching mechanism that adds to the passive galaxy population, with the possible exception of rich cluster cores. We find in addition new relationships for starburst galaxies: the poststarburst/passive fraction is approximately constant at  $\sim 10\%$  over all environments, from isolated galaxies, through groups, to cluster cores, and the active-starburst/continuously-star-forming fraction constant at  $\sim 25\%$ . From this we suggest that mild-to-moderate starbursts in this era are the result of mergers, mostly minor mergers and accretions, specifically, that readily identified active starbursts are events in previously continuously star forming galaxies, to which they will generally return, and poststarbursts are events occurring in previously passive galaxies, to which they will usually return. These events are thought not to fundamentally change the galaxy, except perhaps in the building of larger bulges in disk galaxies. By adding to



this explanation of the starburst phenomenon the popular notion that strangulation and stripping — comparatively slow, environmentally sensitive quenching mechanisms — are mainly responsible for building the higher passive fractions of groups and clusters, we complete a picture which is roughly consistent with what is known about intermediate-redshift galaxy populations, in the full range of environment.

#### 6. ACKNOWLEDGMENTS

Dressler and Oemler acknowledge the support of the NSF grant AST-0407343. All the authors thank NASA for its support through NASA-JPL 1310394. The authors thank Dr. Lori Lubin for helpful discussions and, in particular, Dr. Kristian Finlator, for a provocative comment that led to the interpretation of starbursts presented in this paper.

TABLE 1  
CLUSTER PROPERTIES

ID	RA	DEC	z	N	$\sigma_0$ km s <sup>-1</sup>	$R_{virial}$ Mpc	PAS	CSF	SBH	PSB	SBO
RCS0221A	35.41530	-3.77685	0.430924	247	896	1.27	85	121	27	9	5
RCS1102B	165.67800	-3.66588	0.385657	275	698	1.39	107	137	19	8	3
SDSS0845A	131.36600	3.45924	0.329637	278	1436	1.43	132	109	17	12	7
SDSS1500A	225.14300	1.89275	0.419252	113	637	1.17	47	43	16	3	4
SDSS1500B	225.09400	1.85731	0.517742	160	1398	1.23	53	83	14	5	5

TABLE 2  
CLUSTER GROUP PROPERTIES

Group ID	N <sub>tot</sub>	RA deg	DEC deg	N <sub>tot</sub>	L <sub>gal</sub>	R <sub>pair</sub> Mpc	$\Delta V_0$ km s <sup>-1</sup>	$\sigma_0$ km s <sup>-1</sup>	PAS %	CSF %	SBH %	PSB %	SBO %	N <sub>ex</sub>	Prob	$\tau_{enc}$
RCS0221A-1A	20	35.3304	-3.7006	41.35	11.42	2.18	541.9	362.0	25.0	70.0	0.0	0.0	5.0	6	3.2E-3	2.8979
RCS0221A-1B	16	35.3493	-3.6811	29.19	6.46	1.65	-1499.3	189.4	25.0	64.3	12.5	0.0	6.3	5	< E-4	3.1898
RCS0221A-2A	14	35.2734	-3.8977	36.48	7.27	1.20	433.3	244.8	21.4	57.1	14.3	0.0	0.0	0	1.3E-3	0.7808
RCS0221A-2B	5	35.2905	-3.8953	12.66	3.02	0.98	1331.3	77.7	0.0	80.0	20.0	0.0	0.0	0	3.0E-4	3.3834
RCS0221A-4	24	35.5511	-3.9102	51.99	15.82	2.14	297.5	349.9	20.8	50.0	29.2	0.0	0.0	0	6.0E-4	2.1564
RCS1102B-1A	20	165.845	-3.605	64.38	12.59	1.08	-42.5	181.3	20.0	60.0	10.0	5.0	5.0	1	6.0E-4	0.4905
RCS1102B-1B	4	165.829	-3.6788	11.64	3.07	0.49	-985.8	158.3	0.0	100.0	0.0	0.0	0.0	4	1.1E-2	0.7794
RCS1102B-2	15	165.499	-3.5894	53.82	13.62	1.75	897.0	385.0	13.3	60.0	20.0	6.7	0.0	6	< E-4	1.1299
RCS1102B-3	12	165.502	-3.7916	48.80	10.70	0.86	268.9	162.7	16.6	75.0	8.3	0.0	0.0	6	6.2E-3	0.3307
RCS1102B-4	13	165.725	-3.8076	36.28	9.29	1.14	-679.6	508.4	9.1	81.8	9.1	0.0	0.0	5	2.0E-4	0.6705
RCS1102B-5	10	165.703	-3.6828	18.73	5.04	0.16	-843.1	335.8	60.0	20.0	0.0	20.0	0.0	7	1.8E-3	0.0027
SDSS0845A-1	18	131.178	3.5366	41.79	17.19	0.89	244.8	280.0	22.2	77.8	0.0	0.0	0.0	4	3.0E-4	0.2596
SDSS0845A-2	6	131.244	3.4757	13.01	3.81	0.48	-3273.8	125.2	16.7	33.3	33.3	0.0	16.7	5	< E-4	0.6167
SDSS1500A-1	8	225.239	1.9881	15.33	7.10	0.67	398.2	169.7	25.0	50.0	25.0	0.0	0.0	2	1.1E-2	0.4538
SDSS1500A-2	6	225.331	1.8750	11.17	6.72	1.08	140.2	199.8	16.6	66.7	16.7	0.0	0.0	0	1.6E-1	2.1561
SDSS1500A-3	13	225.102	1.9919	26.02	12.06	1.00	224.5	305.3	38.5	38.5	15.4	0.0	7.6	2	5.5E-2	0.6070
SDSS1500A-4A	14	225.153	1.8936	24.46	10.18	0.70	-791.1	255.9	50.0	21.4	7.1	14.3	7.2	14	2.0E-4	0.2207
SDSS1500A-4B	6	225.147	1.8926	13.76	4.09	0.90	467.7	236.3	83.3	0.0	16.7	0.0	0.0	5	8.8E-2	0.8434
SDSS1500B-1A	3	225.053	1.7293	13.30	5.58	1.63	2143.3	116.2	33.3	66.7	0.0	0.0	0.0	4	5.6E-3	0.00
SDSS1500B-1B	8	225.026	1.7496	21.84	7.96	1.13	-2895.3	401.2	0.0	75.0	25.0	0.0	0.0	3	< E-4	0.6373
SDSS1500B-2	29	224.952	1.802	107.45	38.67	0.86	-99.8	915.4	37.9	55.2	0.0	6.9	0.0	0	2.3E-1	0.0265
SDSS1500B-3	8	225.126	1.8688	41.17	13.72	0.58	1497.0	476.8	62.4	25.0	12.5	0.0	0.0	10	2.4E-2	0.0389
SDSS1500B-4A	6	225.143	1.738	22.59	5.83	0.88	1960.9	319.1	16.7	66.6	0.0	0.0	16.7	2	< E-4	0.3671
SDSS1500B-4B	3	225.178	1.727	10.08	2.74	1.84	-2440.9	34.0	0.0	66.7	33.3	0.0	0.0	2	1.5E-3	255.7150

<sup>a</sup>R<sub>pair</sub> is a radius calculated by as the mean of the separations of all possible pairs

<sup>b</sup>N<sub>tot</sub> & L<sub>gal</sub> are extrapolated values of the number of galaxies and total luminosity, as described in the text.

TABLE 3  
FIELD GROUP PROPERTIES

Group	N	RA	DEC	z	Ntot	Lgal	$\sigma_0$ km s <sup>-1</sup>	Rpair Mpc	PAS %	CSF %	SBH %	PSB %	SBO %	$\tau_{enc}$ Gyr
RCS0221 1A	13	35.30412	-3.85102	0.3157	21.10	4.05	238.0	1.17	23.1	53.8	15.4	0.0	7.7	1.3353
RCS0221 1B	41	35.27720	-3.80787	0.3257	55.44	16.32	317.0	2.08	24.4	56.1	12.2	2.4	4.9	2.1439
RCS0221 2	17	35.55209	-3.81320	0.3487	25.81	7.21	151.0	1.77	17.6	76.5	5.9	0.0	0.0	5.9574
RCS0221 3	7	35.55083	-3.87912	0.3663	11.88	2.69	174.0	0.83	0.0	71.5	28.5	0.0	0.0	1.158
RCS0221 4	8	35.53390	-3.69391	0.4970	22.50	8.19	223.0	2.12	25.0	50.0	25.0	0.0	0.0	7.9510
RCS0221 5	10	35.46751	-3.63309	0.3969	20.11	4.24	240.0	0.78	10.0	60.0	10.0	0.0	20.0	0.4116
RCS0221 6A	8	35.60182	-3.82601	0.4970	22.50	8.19	223.0	2.12	12.5	50.0	25.0	0.0	12.5	7.9510
RCS0221 6B	13	35.49378	-3.88737	0.5002	35.15	14.51	123.0	2.02	15.4	76.9	0.0	7.7	0.0	7.9822
RCS0221 7	7	35.54801	-3.75429	0.5159	26.01	7.06	295.0	0.85	14.3	85.7	0.0	0.0	0.0	0.3351
RCS1102 1	13	165.53380	-3.60421	0.3424	45.53	9.25	123.0	2.07	15.4	69.2	15.4	0.0	0.0	6.6314
RCS1102 2	15	165.65413	-3.83397	0.3481	38.44	7.65	172.0	2.07	20.0	53.3	20.0	0.0	6.7	5.6169
RCS1102 3	16	165.75301	-3.61600	0.3617	46.32	17.23	204.0	1.47	18.8	62.4	12.5	6.3	0.0	1.4075
RCS1102 4	21	165.50757	-3.74132	0.3667	83.06	22.24	291.0	1.52	23.8	66.7	4.7	4.8	0.0	0.6083
RCS1102 5	24	165.66133	-3.66528	0.3993	86.30	20.82	145.0	2.65	25.0	45.8	25.0	0.0	4.2	6.2267
RCS1102 9	16	165.74455	-3.77131	0.4755	87.68	23.01	109.0	3.11	12.5	68.8	18.7	0.0	0.0	13.1782
RCS1102 10	48	165.67100	-3.73191	0.4992	255.38	82.89	341.0	4.23	35.4	50.0	2.1	10.4	2.	3.6390
SDSS0845 2B	10	131.38068	3.34949	0.3811	30.39	10.33	269.0	2.09	0.0	80.0	10.0	0.0	10.0	4.6758
SDSS0845 3	14	131.25034	3.50936	0.4438	48.28	16.33	157.0	2.39	21.4	64.4	0.0	7.1	7.1	7.5410
SDSS0845 4	7	131.44269	3.57199	0.4545	27.93	6.20	447.0	2.42	14.2	85.8	0.0	0.0	0.0	4.7530
SDSS1500 1	11	225.20789	1.79321	0.3719	19.16	7.51	214.0	1.44	54.6	45.4	0.0	0.0	0.0	3.0491
SDSS1500 3	8	225.31461	1.90860	0.3955	12.90	4.43	302.0	1.60	25.0	37.5	25.0	12.5	0.0	4.4021
SDSS1500 5	14	225.22456	2.00235	0.4577	32.26	11.65	212.0	2.25	21.4	42.8	21.4	7.2	7.2	6.9734
SDSS1500 6	9	225.13403	1.95897	0.4799	19.80	4.05	262.0	2.85	11.1	55.6	22.2	11.1	0.0	18.6840

TABLE 4  
FIELD FILAMENT PROPERTIES

Group	N	RA	DEC	z	Ntot	Lgal	$\sigma_0$ km s <sup>-1</sup>	Rpair Mpc	PAS %	CSF %	SBH %	PSB %	SBO %	$\tau_{enc}$ Gyr
RCS1102 6	8	165.72307	-3.84014	0.4265	30.24	9.96	287.0	1.88	25.0	62.5	12.5	0.0	0.0	3.2056
RCS1102 7	15	165.73518	-3.65126	0.4424	48.53	19.02	165.0	2.75	20.0	80.0	0.0	0.0	0.0	10.8744
RCS1102 8	11	165.69684	-3.56506	0.4741	50.53	10.28	278.0	3.14	9.1	81.8	9.1	0.0	0.0	9.2277
SDSS0845 1	11	131.4595	3.52035	0.3580	25.00	5.18	169.0	1.73	9.1	72.7	18.2	0.0	0.0	5.1311
SDSS0845 2A	8	131.36554	3.35107	0.3647	17.97	5.51	203.0	2.10	0.0	100.0	0.0	0.0	0.0	10.6295
SDSS1500 2	14	225.10097	1.83667	0.3775	25.59	11.28	187.0	2.59	57.1	42.9	0.0	0.0	0.0	15.2016
SDSS1500 7	15	225.08087	1.72892	0.4835	40.31	11.43	345.0	2.48	26.7	53.3	13.3	0.0	6.7	4.5922

## REFERENCES

- Abadi, M. G., Moore, B., & Bower, R. G. 1999, *MNRAS*, 308, 947
- Balogh, M. L., Morris, S. L., Yee, H. K. C., Carlberg, R. G., & Ellingson, E. 1999, *ApJ*, 527, 54
- Balogh, M. L., McGee, S. L., Wilman, D., et al. 2009, *MNRAS*, 398, 754
- Balsara, D., Livio, M., & O’Dea, C. P. 1994, *ApJ*, 437, 83
- Barger, A. J., Aragon-Salamanca, A., Ellis, R. S., et al. 1996, *MNRAS*, 279, 1
- Bekki, K. 1998, *ApJ*, 502, L133 — unequal mergers of gas rich spirals as a method of S0 production
- Bekki, K. 2001, *Ap&SS*, 276, 847
- Bekki, K., Couch, W. J., & Shioya, Y. 2002, *ApJ*, 577, 651
- Bekki, K., & Couch, W. J. 2003, *ApJ*, 596, L13
- Bekki, K., Couch, W. J., Shioya, Y., & Vazdekis, A. 2005, *MNRAS*, 359, 949 — major mergers form poststarbursts
- Bekki, K. 2009, *MNRAS*, 399, 2221 — ram-pressure stripping of outer gas, difference in clusters and groups, slower evolution
- Bekki, K., Owers, M. S., & Couch, W. J. 2010, *ApJ*, 718, L27
- Bekki, K., & Couch, W. J. 2011, *MNRAS*, 415, 1783 — slow tidal encounters in groups make S0’s
- Berrier, J. C., Stewart, K. R., Bullock, J. S., et al. 2009, *ApJ*, 690, 1292
- Boselli, A., & Gavazzi, G. 2006, *PASP*, 118, 517
- Boselli, A., Boissier, S., Cortese, L., et al. 2006, *ApJ*, 651, 811
- Brown, M. J. I., Dey, A., Jannuzi, B. T., et al. 2007, *ApJ*, 654, 858
- Carlberg, R. G., Yee, H. K. C., Morris, S. L., et al. 2001, *ApJ*, 552, 427
- Cortese, L., Gavazzi, G., Boselli, A., et al. 2006, *A&A*, 453, 847
- Couch, W. J., & Sharples, R. M. 1987, *MNRAS*, 229, 423
- De Filippis, E., & Schindler, S. 2003, *Ap&SS*, 285, 167
- De Lucia, G., Poggianti, B. M., Halliday, C., et al. 2009, *MNRAS*, 400, 68
- De Lucia, G., Weinmann, S., Poggianti, B., Aragon-Salamanca, A., & Zaritsky, D. 2011, arXiv:1111.6590
- Desai, V., Dalcanton, J. J., Aragón-Salamanca, A., et al. 2007, *ApJ*, 660, 1151
- Dressler, A. 1976, PhD Thesis, University of California, Santa Cruz
- Dressler, A. 1980, *ApJ*, 236, 351
- Dressler, A., & Gunn, J. E. 1983, *ApJ*, 270, 7
- Dressler, A. 1986, *ApJ*, 301, 35
- Dressler, A., & Shectman, S. A. 1988, *AJ*, 95, 985
- Dressler, A., Oemler, A., Jr., Couch, W. J., et al. 1997, *ApJ*, 490, 577
- Dressler, A., Smail, I., Poggianti, B. M., et al. 1999, *ApJS*, 122, 51
- Dressler, A., Oemler, A., Jr., Poggianti, B. M., et al. 2004, *ApJ*, 617, 867
- Dressler, A., Oemler, A., Gladders, M. G., et al. 2009a, *ApJ*, 699, L130
- Dressler, A., Rigby, J., Oemler, A., Jr., et al. 2009b, *ApJ*, 693, 140
- Ellingson, E., Lin, H., Yee, H. K. C., & Carlberg, R. G. 2001, *ApJ*, 547, 609
- Faber, S. M., Willmer, C. N. A., Wolf, C., et al. 2007, *ApJ*, 665, 265
- Geller, M. J., & Beers, T. C. 1982, *PASP*, 94, 421
- Gladders, M. D., Oemler, A., Jr. 2012, in preparation
- Gladders, M. D., & Yee, H. K. C. 2005, *ApJS*, 157, 1
- Gunn, J. E., & Gott, J. R., III 1972, *ApJ*, 176, 1
- bibitem[Just et al.(2010)]2010ApJ...711..192J Just, D. W., Zaritsky, D., Sand, D. J., Desai, V., & Rudnick, G. 2010, *ApJ*, 711, 192 (S0 evolution — preprocessing)
- A
- Just, D. W., Zaritsky, D., Tran, K.-V. H., et al. 2011, *ApJ*, 740, 54 (Supergroup)
- Kapferer, W., Kronberger, T., Ferrari, C., Riser, T., & Schindler, S. 2008, *MNRAS*, 389, 1405
- Kapferer, W., Sluka, C., Schindler, S., Ferrari, C., & Ziegler, B. 2009, *A&A*, 499, 87
- Kauffmann, G. 1995, *MNRAS*, 274, 153
- Kelson, D. D., Illingworth, G. D., Franx, M., & van Dokkum, P. G. 2001, *ApJ*, 552, L17
- Kodama, T., Tanaka, M., Tamura, T., et al. 2005, *PASJ*, 57, 309
- Larson, R. B., Tinsley, B. M., & Caldwell, C. N. 1980, *ApJ*, 237, 692
- Lemaux, B. C., Lubin, L. M., Shapley, A., et al. 2010, *ApJ*, 716, 970
- Lynden-Bell, D. 1967, *MNRAS*, 136, 101
- McGee, S. L., Balogh, M. L., Bower, R. G., Font, A. S., & McCarthy, I. G. 2009, *MNRAS*, 400, 937
- Mihos, J. C. 2004, *Clusters of Galaxies: Probes of Cosmological Structure and Galaxy Evolution*, 277
- Moore, B., Lake, G., & Katz, N. 1998, *ApJ*, 495, 139
- Moran, S. M., Ellis, R. S., & Treu, T. 2008, *Panoramic Views of Galaxy Formation and Evolution*, 399, 344
- Oemler, A., Jr., Dressler, A., & Butcher, H. R. 1997, *ApJ*, 474, 561
- Oemler, A., Jr., Dressler, A., Kelson, D., et al. 2009, *ApJ*, 693, 152
- Oemler, A., Jr., Dressler, A., Gladders, M. G., Rigby, J. R., Bai, L., Kelson, D., Villaneuva, E., Fritz, J., Poggianti, B. M., & Vulcani, V. 2012a, submitted to *ApJ* — Paper 1
- Oemler, A., Jr., Dressler, A., Gladders, M. G., Fritz, J., & Poggianti, B. M. 2012b, submitted — Paper 2
- Peng, Y.-j., Lilly, S. J., Kovač, K., et al. 2010, *ApJ*, 721, 193
- Poggianti, B. M., Smail, I., Dressler, A., et al. 1999, *ApJ*, 518, 576
- Poggianti, B. M. 2004, *Clusters of Galaxies: Probes of Cosmological Structure and Galaxy Evolution*, 245
- Poggianti, B. M., von der Linden, A., De Lucia, G., et al. 2006, *ApJ*, 642, 188
- Poggianti, B. M., Desai, V., Finn, R., et al. 2008, *ApJ*, 684, 888
- Poggianti, B. M., Aragón-Salamanca, A., Zaritsky, D., et al. 2009, *ApJ*, 693, 112
- Postman, M., Franx, M., Cross, N. J. G., et al. 2005, *ApJ*, 623, 721
- Quilis, V., Moore, B., & Bower, R. 2000, *Science*, 288, 1617
- Richstone, D. O. 1976, *ApJ*, 204, 642
- Schechter, P. 1976, *ApJ*, 203, 297
- Springel, V. et al. 2005, *Nature*, 435, 629
- Tran, K.-V. H., Franx, M., Illingworth, G., Kelson, D. D., & van Dokkum, P. 2003, *ApJ*, 599, 865
- van den Bosch, F. C., Aquino, D., Yang, X., et al. 2008, *MNRAS*, 387, 79
- van Dokkum, P. G., Franx, M., Fabricant, D., Illingworth, G. D., & Kelson, D. D. 2000, *ApJ*, 541, 95
- van Dokkum, P. G., Franx, M., Kriek, M., et al. 2008, *ApJ*, 677, L5
- Weinmann, S. M., Kauffmann, G., von der Linden, A., & De Lucia, G. 2010, *MNRAS*, 406, 2249
- White, S. D. M. 1976, *MNRAS*, 177, 717
- Wild, V., Walcher, C. J., Johansson, P. H., et al. 2009, *MNRAS*, 395, 144
- Williams, R. J., Quadri, R. F., Franx, M., et al. 2010, *ApJ*, 713, 738
- Wilman, D. J., Oemler, A., Jr., Mulchaey, J. S., et al. 2009, *ApJ*, 692, 298
- Zabludoff, A. I., Zaritsky, D., Lin, H., et al. 1996, *ApJ*, 466, 104

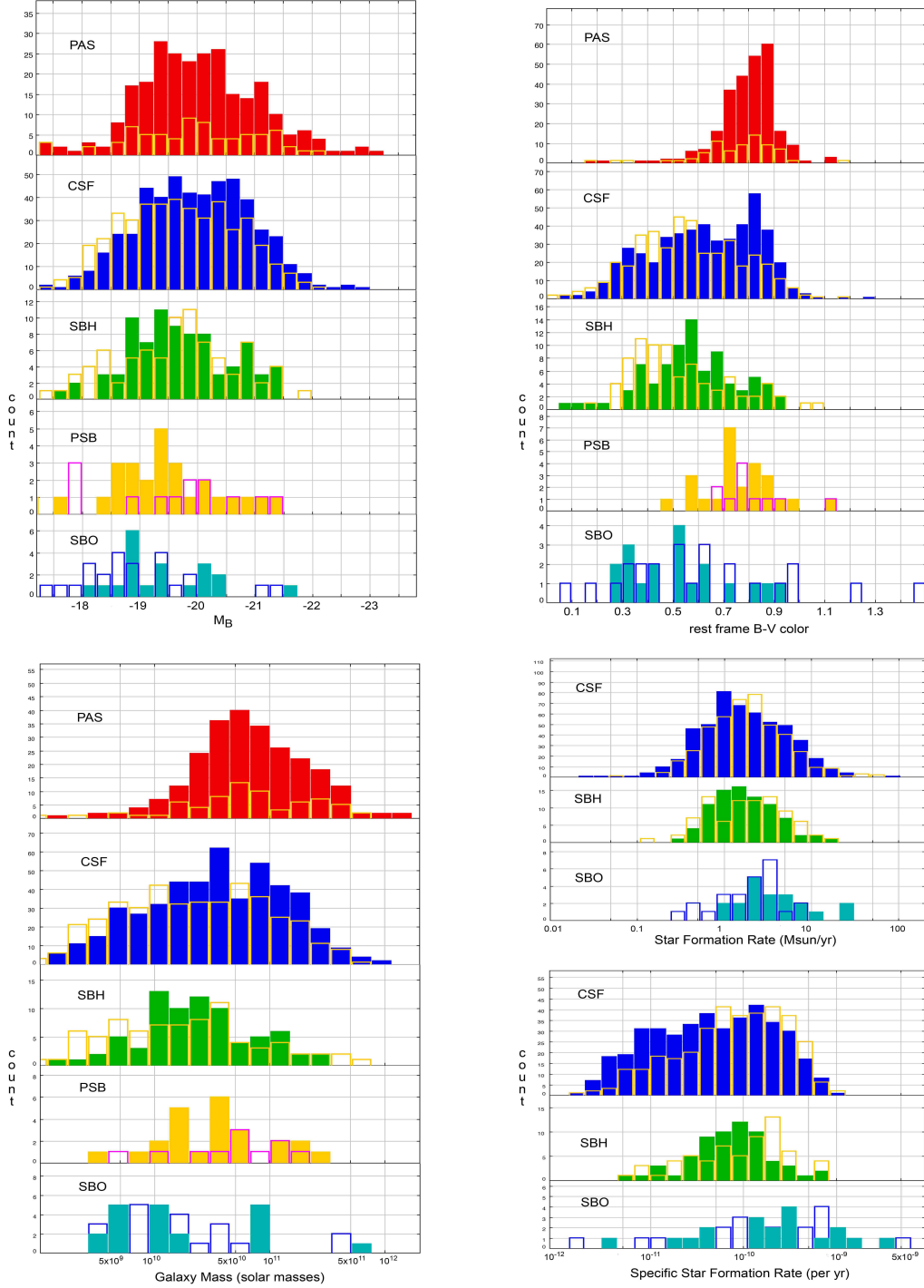


FIG. 1.— Solid histograms: Distributions of (a)  $M_B$  luminosity, (b) rest-frame B-V color, and (c) galaxy mass, for ICBS cluster galaxies for the five spectral types, for 915 members of the clusters of RCS0221A, RCS1102B, SDSS0845A, & SDSS 1500A. (SDSS1500B has excluded because its higher redshift results in significant faint-end incompleteness.) Open histograms: the same quantities for 1090 field galaxies in the redshift range  $0.31 < z < 0.54$  covered by the clusters. PAS galaxies reach to higher luminosities and mass, and have a small range of red color, as is conventionally found. However, despite a very different B-V color (and ergo stellar population) distribution, CSF galaxies at  $z \sim 0.4$  overlap substantially with PAS galaxies and reach masses nearly as high. SBH and SBO (active) starburst galaxies are generally bluer than even CSF galaxies, as might be expected, while PSB galaxies are clearly on the way to match the red and narrow PAS color distribution. The SBH, SBO, and PSB galaxies are typically a factor of 2-3 less massive than PAS or CSF galaxies. Star formation rates for CSF, SBH, and SBO galaxies cover a very similar range (top of d), but a distinct difference is seen in terms of sSFRs (specific SFRs), with SBH galaxies having somewhat greater sSFRs and SBO galaxies very noticeably shifted to higher values.

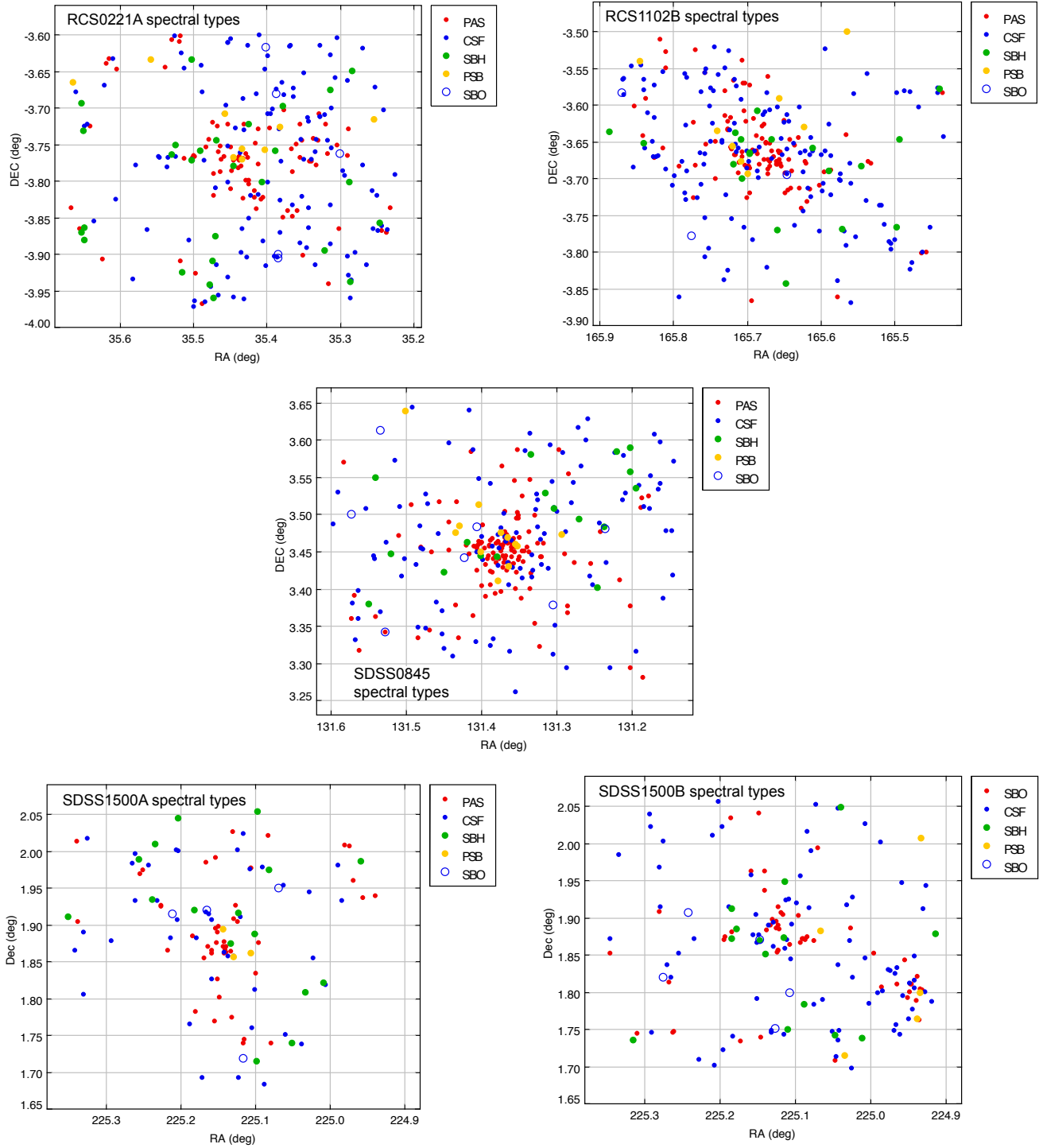


FIG. 2.— Sky maps of ICBS clusters showing the distribution of spectral types. Passive galaxies (PAS) are strongly concentrated to the cluster center or dense outer groups. poststarburst galaxies (PSB) trace the PAS population. Continuously-star-forming galaxies are more uniformly distributed, as are the active starbursts, SBH (strong Balmer absorption lines) and SBO (strong [O II] emission).

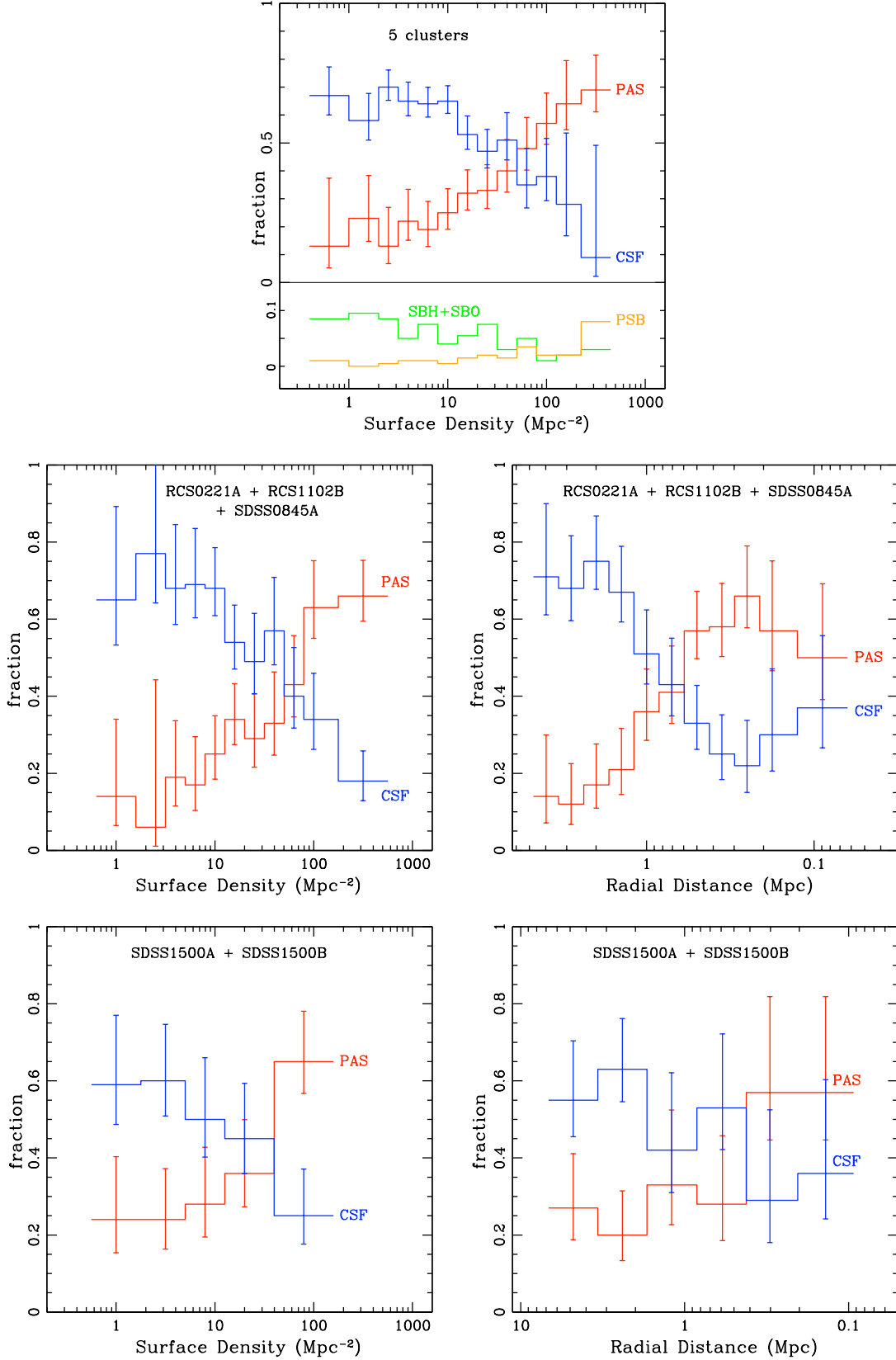


FIG. 3.— a) Spectral-type fractions vs. surface density for the full 5-cluster sample. The upper panel shows the strong behavior of PAS (passive) and CSF (continuously starforming) galaxies, which closely resembles morphology-density relations (Dressler 1980; Dressler et al. 1997). The bottom panel shows that the active starbursts decline in proportion with the CSF galaxies and the PSB rise in proportion to the PAS galaxies, a feature that suggests a pairing of PAS to PSB and (SBH+SBO) to CSF spectral types. b) Spectral-type fractions relation for 3 concentrated, regular clusters. c) Spectral-type fractions vs. clustocentric radius for 3 concentrated clusters. d) Spectral-type fractions vs. surface density relation for 2 irregular clusters composed mainly of rich groups. e) Same as (d) for spectral-type fractions vs. clustocentric radius, showing a weaker relation for this compared to (c) and (d).

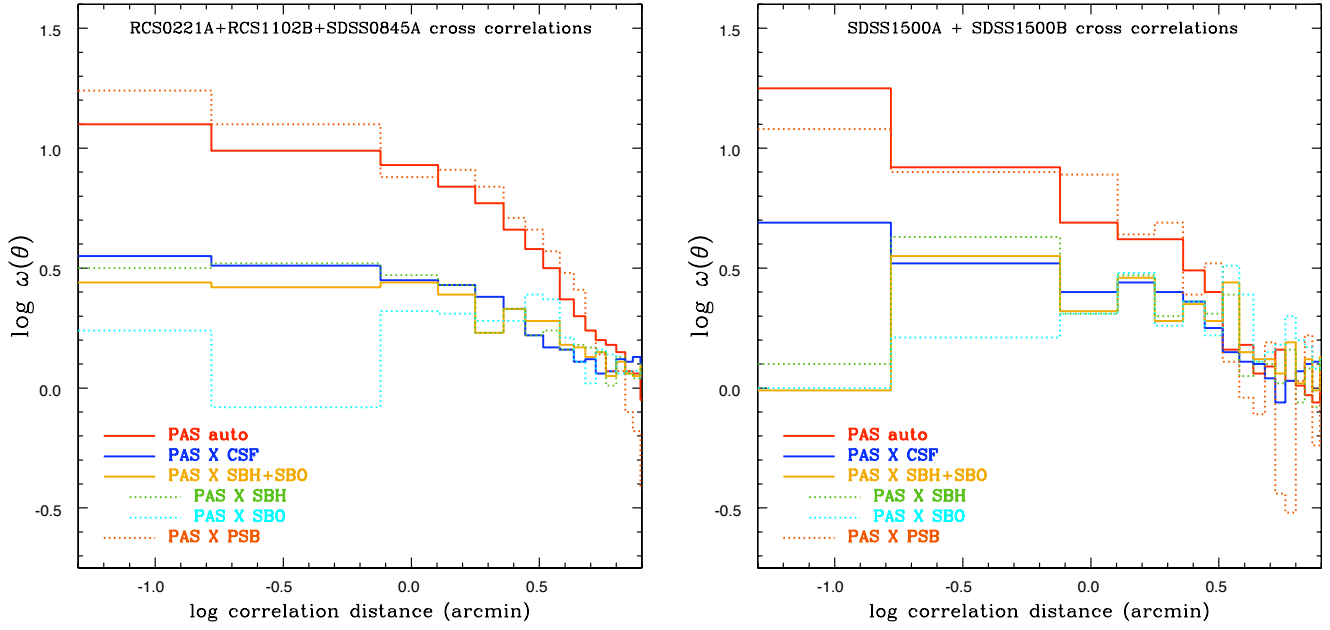


FIG. 4.— Angular cross-correlation of different spectral types. a) (left) The clustering strength of active starbursts, SBH+SBO, matches the clustering of continuously star forming systems in these three “regular” clusters, RCS0221A, RCS1102B, and SDSS0845A. Similarly, post starburst (PSB) galaxies are as strongly clustered as the passive (PAS) members of the population, which could indicate that decaying starbursts are adding to the passive galaxies in the clusters. b) (right) The same of spatial distribution of PSB tracing PAS, and SBH+SBO tracing CSF as seen in (a), for two less concentrated, more irregular clusters, SDSS1500A and SDSS1500B, showing the same results as for the regular clusters.



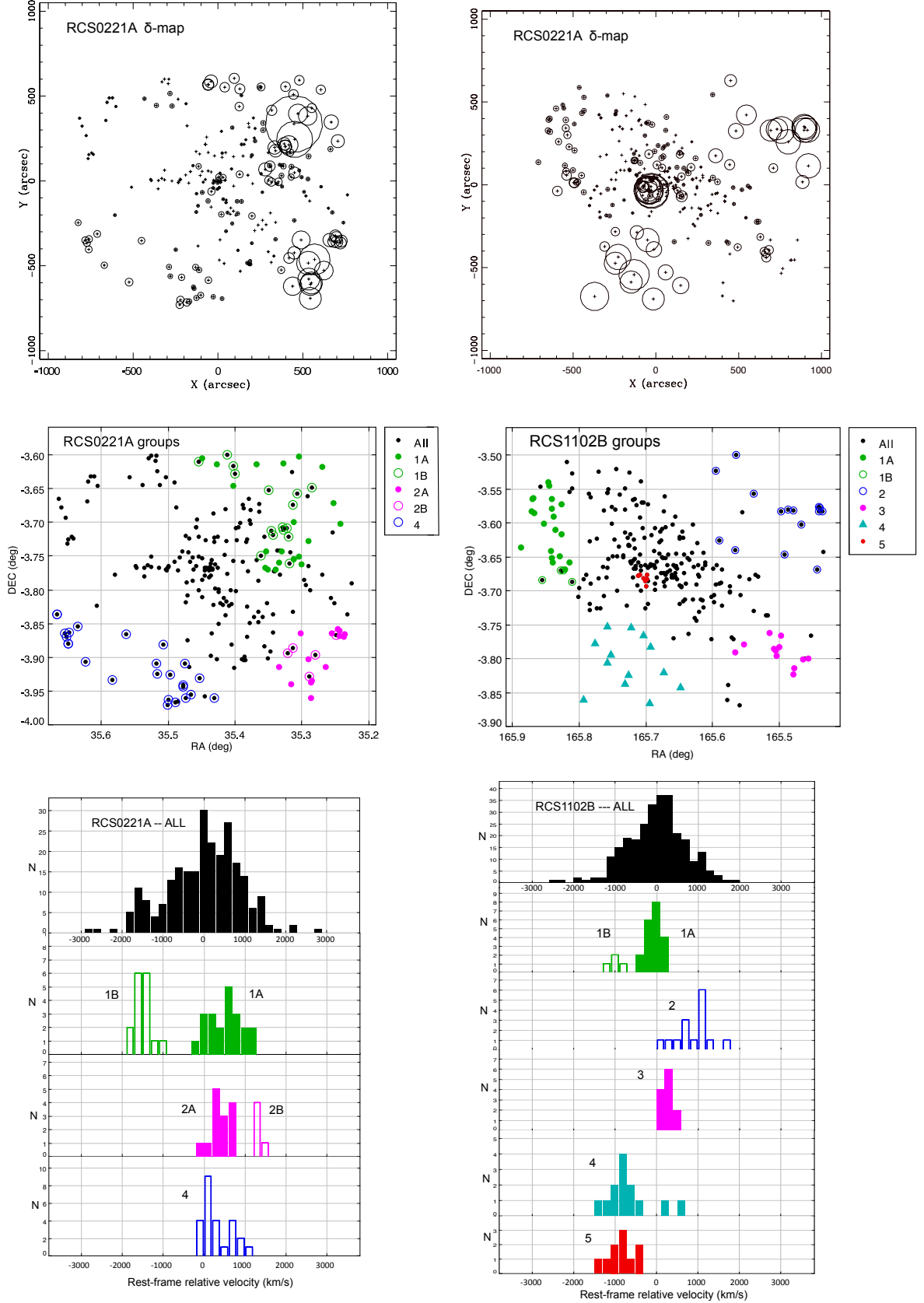


FIG. 5.— Groups in the RCS0221A and RCS1102B clusters. left, RCS0221A: (a) “delta plot” (top), (b) map (middle), (c) velocity histograms. right, RCS1102B: (d) “delta plot” (top), (e) map (middle), (f) member velocity histograms (bottom).

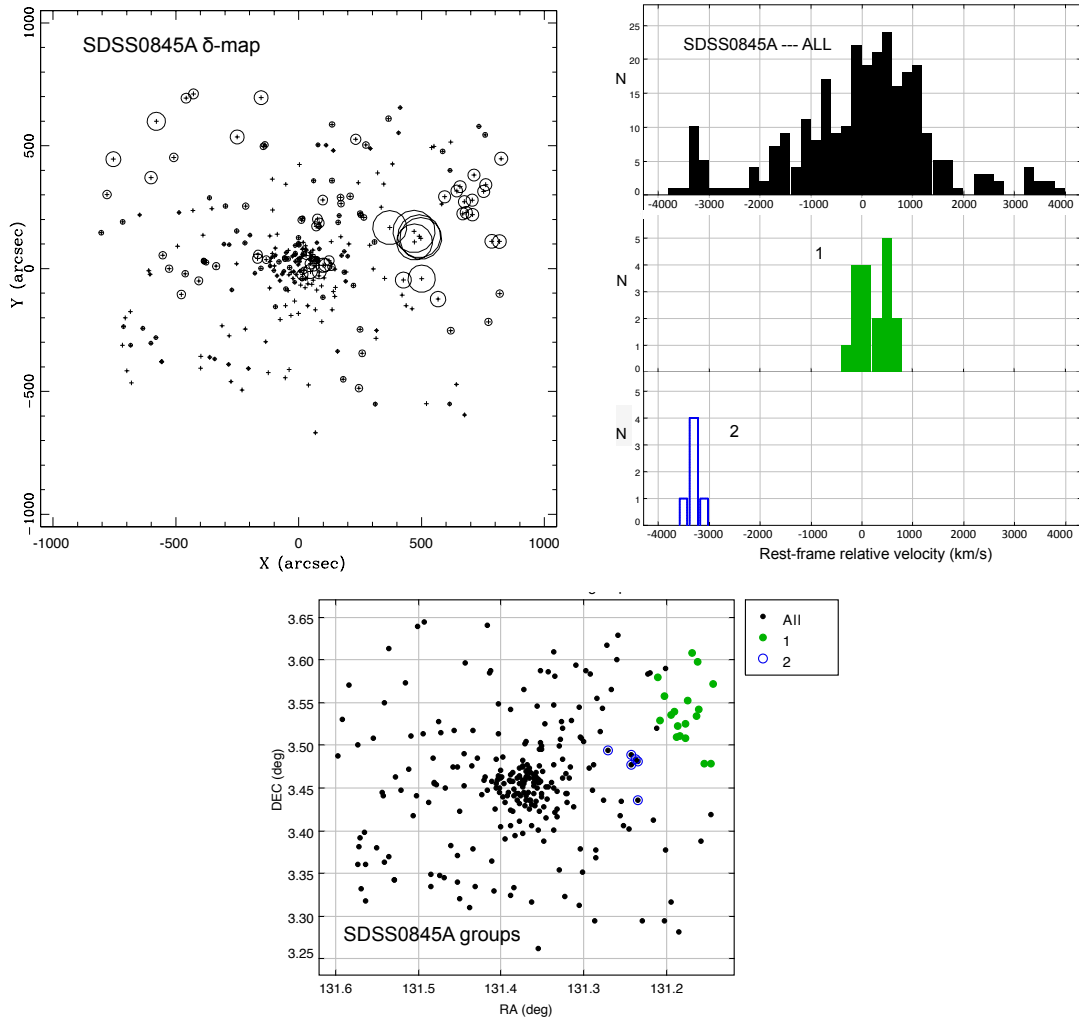


FIG. 6.— Groups in the SDSS0845A cluster. (a) “delta plot” (top-left), (b) map (bottom), (c) member velocity histograms (top-right)

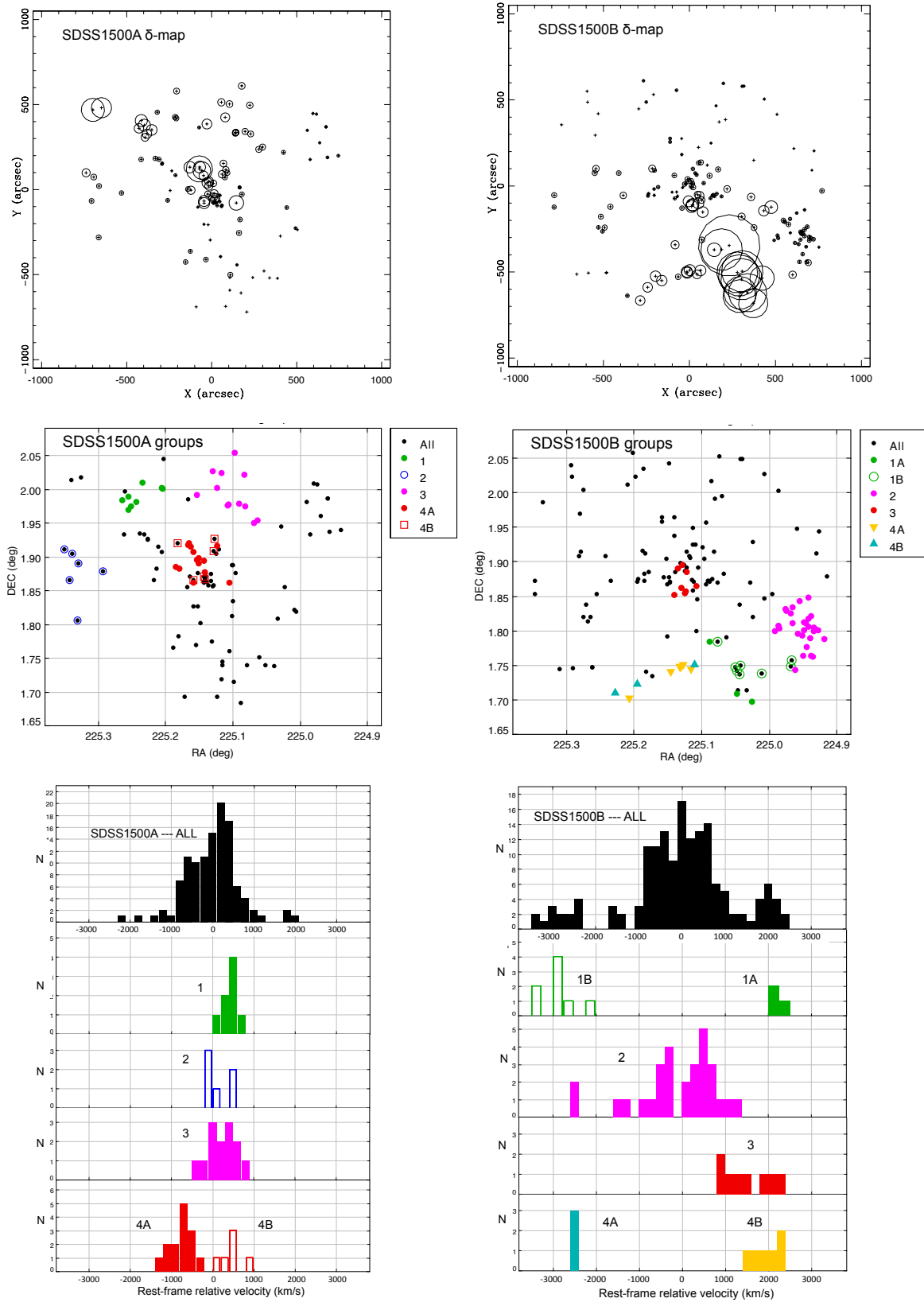


FIG. 7.— Groups in the SDSS1500A and SDSS1500B clusters. left, SDSS1500A: (a) “delta plot” (top), (b) map (middle), (c) velocity histograms. right, SDSS1500B: (d) “delta plot” (top), (e) map (middle), (f) member velocity histograms (bottom).

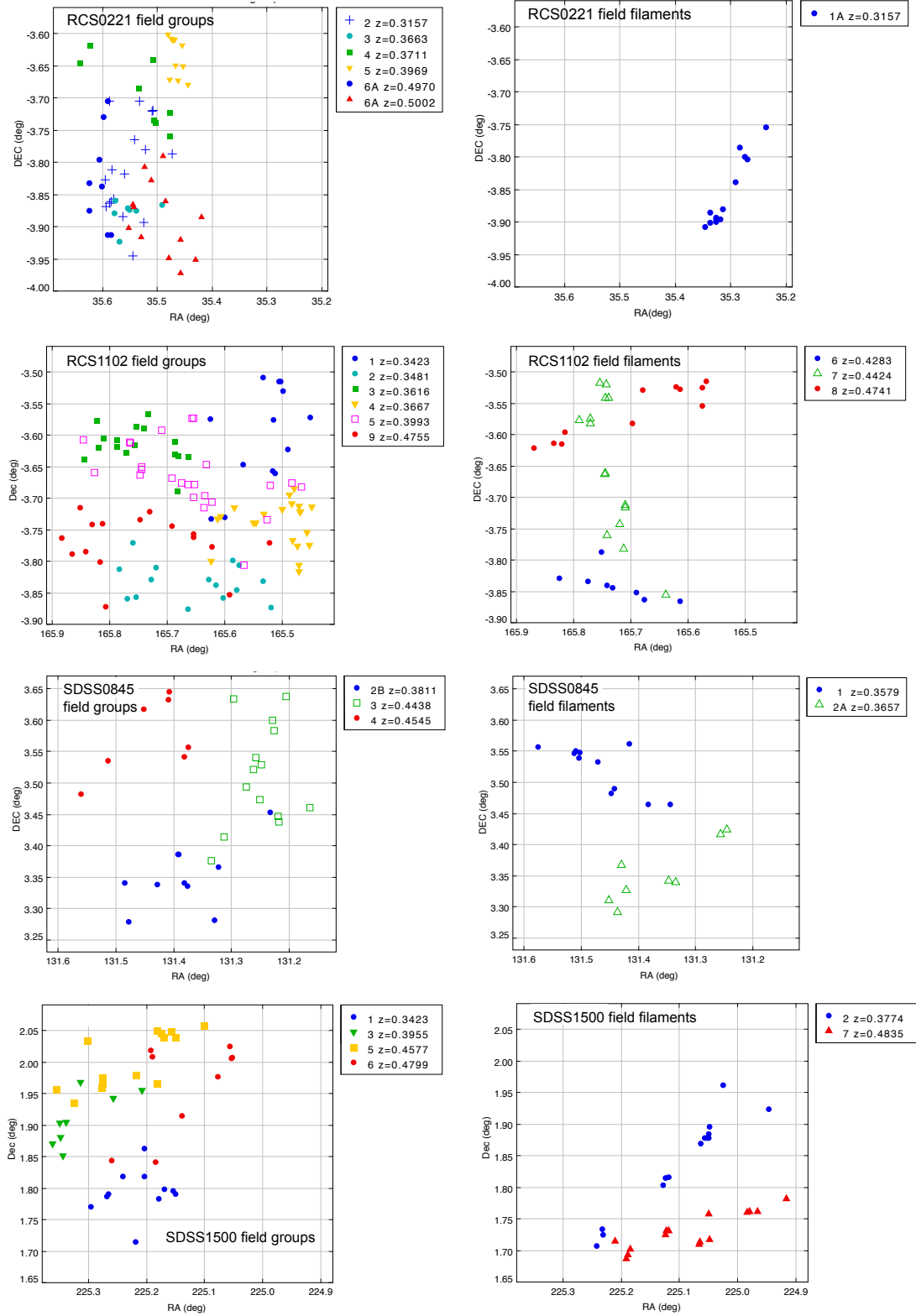


FIG. 8.— Structures in the field  $0.31 < z < 0.54$  that resemble — in number and spatial extent — the infalling groups found in the 5 rich clusters. The left panels show the analogous groups while the right panels show filamentary structures, chosen on purely morphological grounds, that are not found in the ICBS cluster sample of groups.

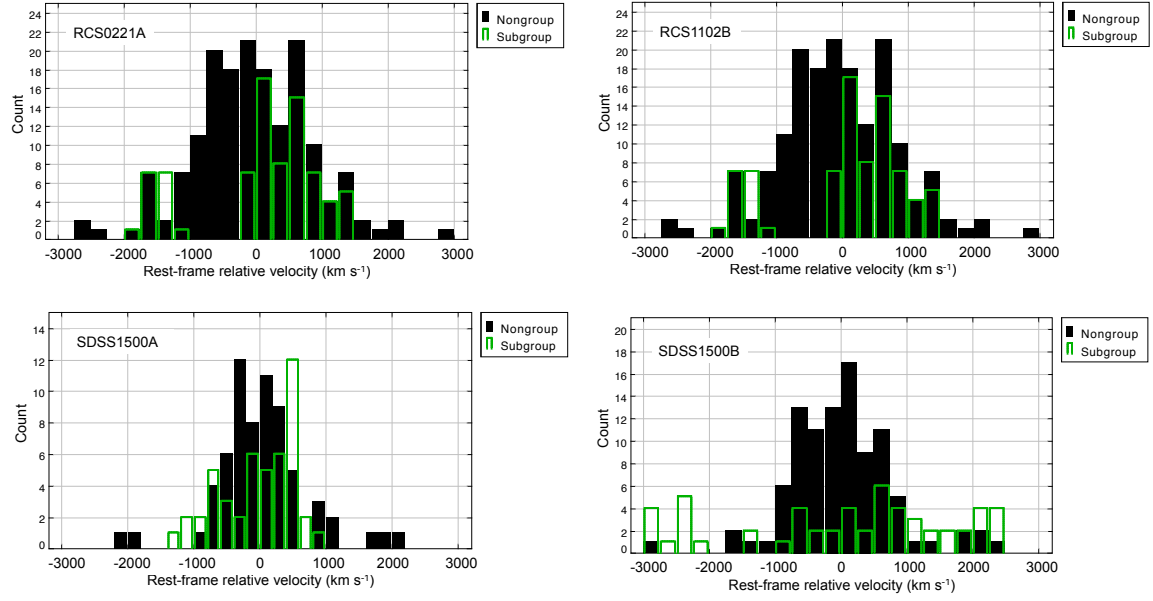


FIG. 9.— Comparison of the velocity histograms for the group members (green) compared to the remaining cluster members (black) for RCS0221A, RCS1102B, SDSS1500A, & SDSS1500B. The groups share the dynamical properties of the previously assembled cluster, demonstrating that they are both sampling the same gravitational potential and that individual groups can have very high infall velocities, even when the radial component is not included.

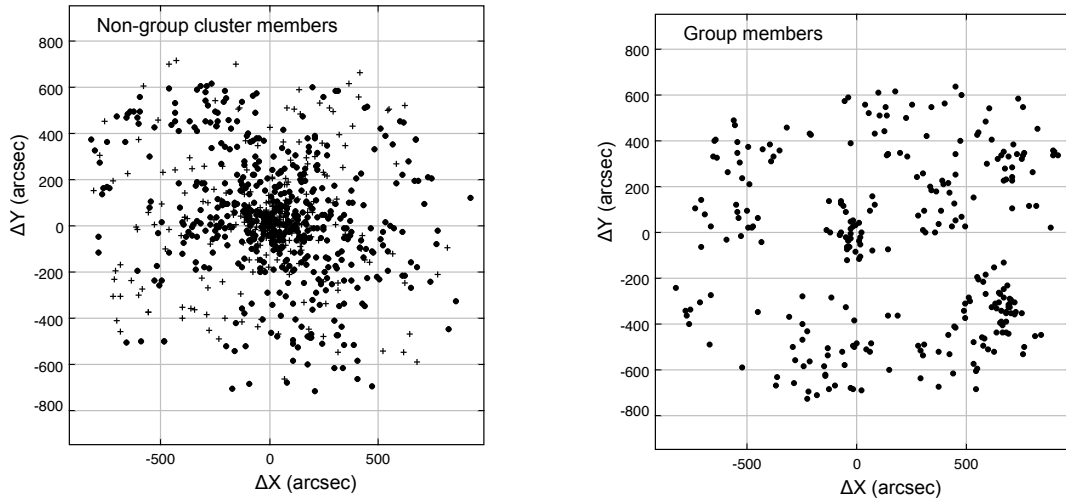


FIG. 10.— Composite ‘sky maps’ of cluster members. a) (left) closed dots – cluster members not in groups in RCS0221A, RCS1102B, SDSS1500A & B; plus signs – SDSS0845 non-group members. b) (right) closed dots – members of cluster groups for all 5 clusters.

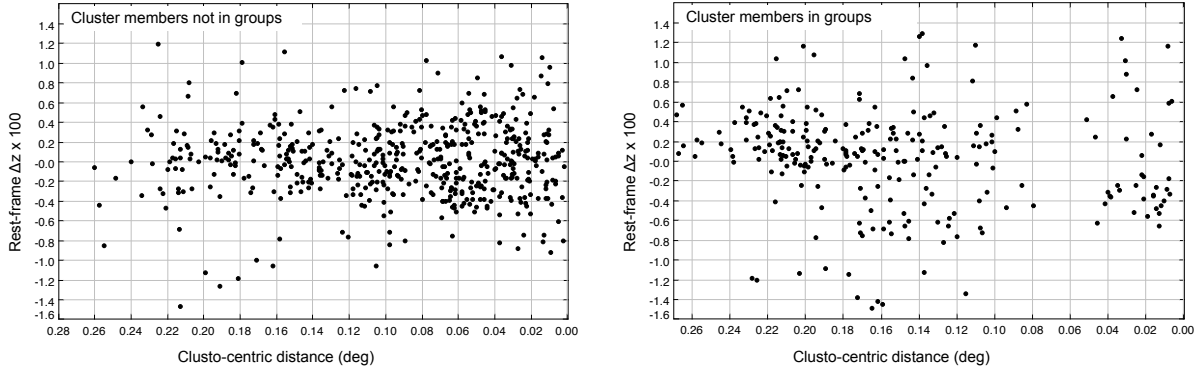


FIG. 11.— Delta redshift from the mean cluster velocity as a function of Rcl, for four clusters — RCS0221A + RCS1102B + SDSS1500A + SDSS1500B — for members of these clusters not in groups (left) and for cluster members in groups (right).

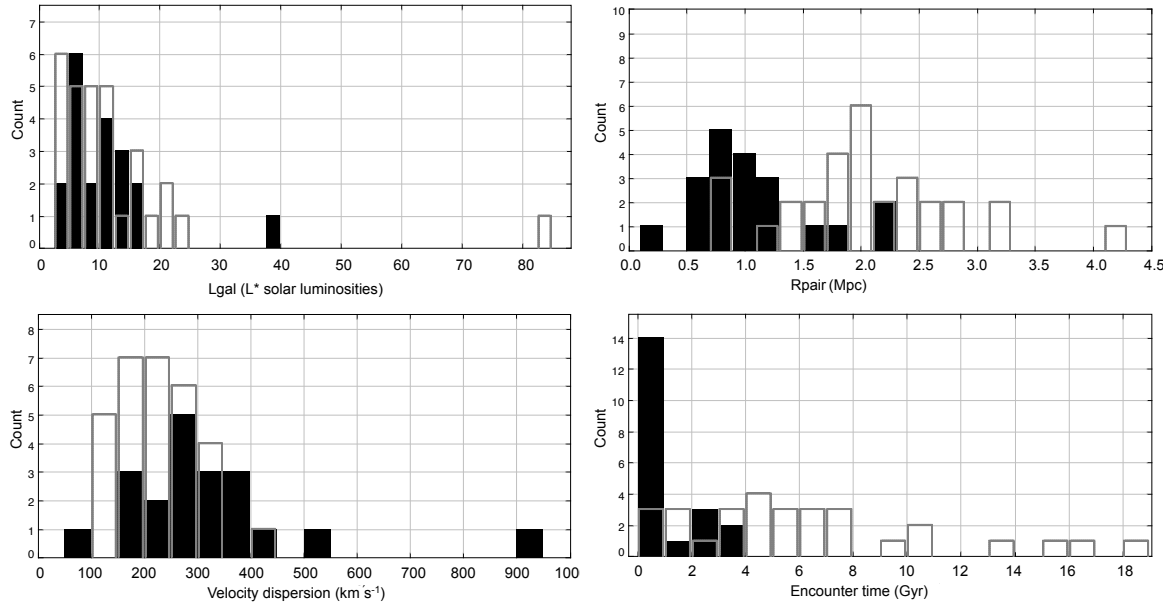


FIG. 12.— Properties of the cluster groups, and field groups and filaments. Cluster groups — solid histogram; field groups and filaments — open histogram. (upper-left) Group luminosity; b) (upper-right) group radius in Mpc; c) (lower-left) group velocity dispersion; d) (lower-right) group encounter time. The distribution of number of members (not shown) is very similar for the cluster and field groups, as is mirrored in the distribution of Lgal upper left. The velocity dispersions of the cluster and field groups are also very similar, though the cluster sample contains a significant number of higher-dispersion systems. More distinct, however, is the difference in sizes: field groups extend to substantially larger sizes, which accounts for the larger “encounter times” — the characteristic time in Gyr for a group member to encounter a neighbor.

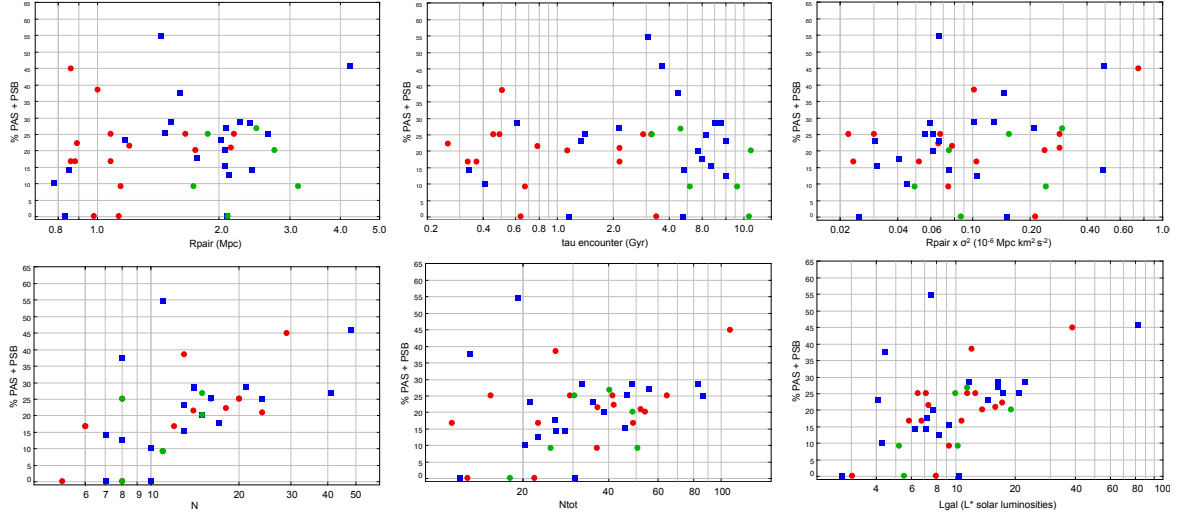


FIG. 13.— Dependence of fraction of passive galaxies, PAS+PSB on various properties of the cluster and field groups and filaments. The figures have been roughly ordered by the strength of the correlation. (a-c) There is no significant correlation of the passive fraction on group size  $R_{pair}$  — a measure of group size (top-left), or for  $\tau_{enc}$  — a typical time for any galaxy to encounter another group member (top-middle). There seems to be a weak correlation of  $R_{pair} \times \sigma^2$  — a measure of group dynamical mass (top-right). (d-f) Significant correlations are found with parameters describing the “richness” or “scale” of the group, for a simple number count  $N$  (bottom-left), and the parameter  $N_{tot}$  that is corrected for the different depths to which the groups are probed (bottom-middle). The best correlation (bottom-right) is with cluster luminosity,  $L_{gal}$ , closely related to cluster mass, by a modest correction for the average mass-to-light ratio for the group. This final relationship is explored in more detail in Figure 14.

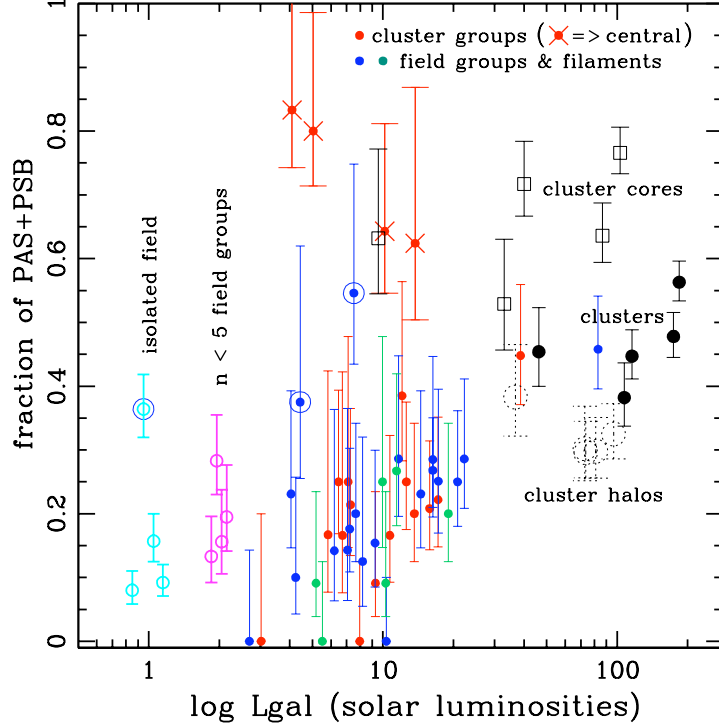


FIG. 14.— Fraction of PAS+PSB spectral type galaxies as a function of  $L_{gal}$ , the total galaxy luminosity, used as a proxy for group mass. The cluster groups (red dots), field groups (blue dots), and field filaments (green dots) all show a trend of increasing PAS+PSB fraction with increasing  $L_{gal}$ , one that continues on to the points for “clusters minus groups” (black dots), as explained in the text. Also on the extrapolation of the trend for typical groups ( $N \sim 10-15$ ) are two rich groups — one cluster and one field — within a factor of  $\sim 2$  of the same  $L_{gal}$  as the cluster values. Also shown are less populous groups ( $N < 5$ ) field identified with a friends-of-friends algorithm (open magenta circles), and isolated field galaxies (open cyan circles). The “clusters minus group” populations have been decomposed into “core” and “halo” populations, split at the virial radius of each cluster, as marked by the labels. The data support a picture in which a “floor” of  $\sim 10\%$  PAS+PSB galaxies, for isolated galaxies and small groups, grows as more massive groups are assembled. Such “pre-processing” in groups favors galaxy-galaxy interactions, a mechanism that is favored in the group environment, but galaxy starvation may also be important. Ram-pressure stripping should not be effective in groups, but it does appear to be in the dense cores of rich clusters.

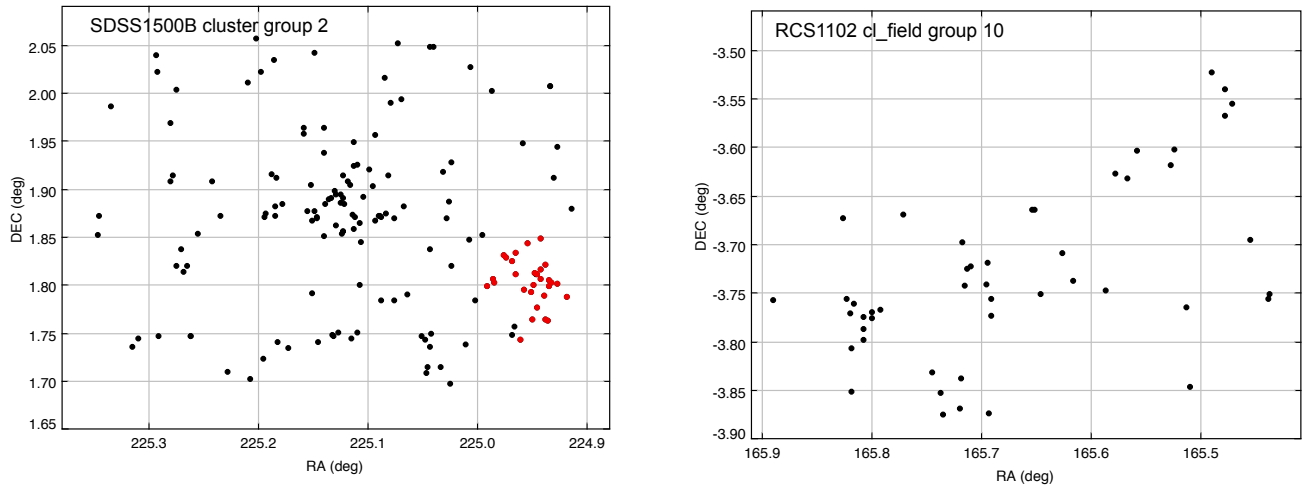


FIG. 15.— Two rich groups, Group 2 in the cluster SDSS1500B, and Group 10 ( $z=0.4992$ ) in the field of the cluster RCS1102B ( $z=0.3857$ ). The two groups have similar richness ( $N_{\text{tot}}$  and  $L_{\text{gal}}$ ) and spectral type distribution (see Figure 14), but are very different in structure. The PAS (open circles) and PSB (open triangles) are widely distributed in SDSS1500B cluster group 2.



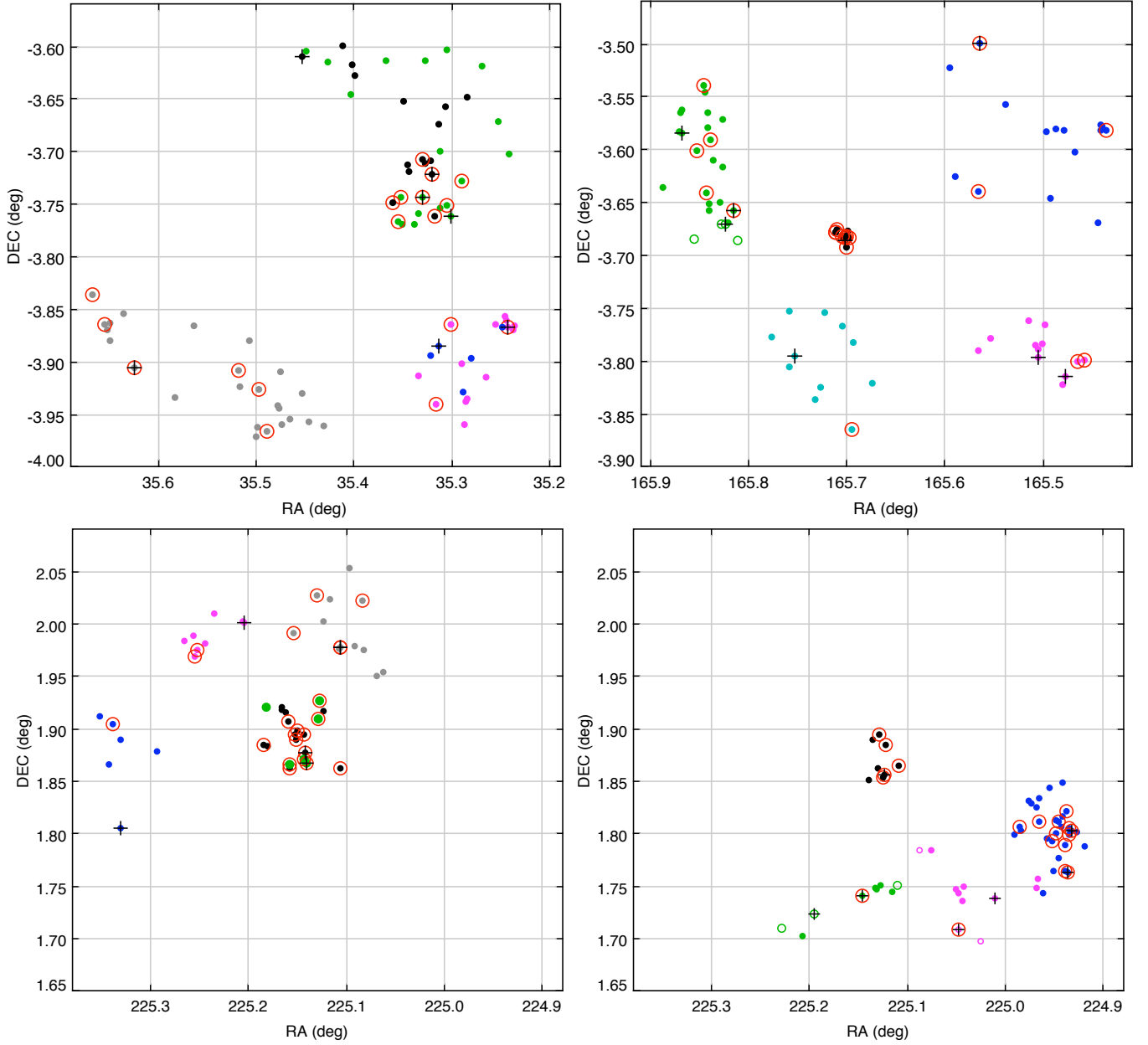


FIG. 16.— Identification of PAS and PSB spectral type galaxies in the cluster groups, marked by open circles. These types are found in locally dense environments, consistent with the idea that incorporation into a larger halo system ends star formation in a “satellite” galaxy, but they also fairly common in low-density or even isolated environments where no such more-massive companion can be responsible.

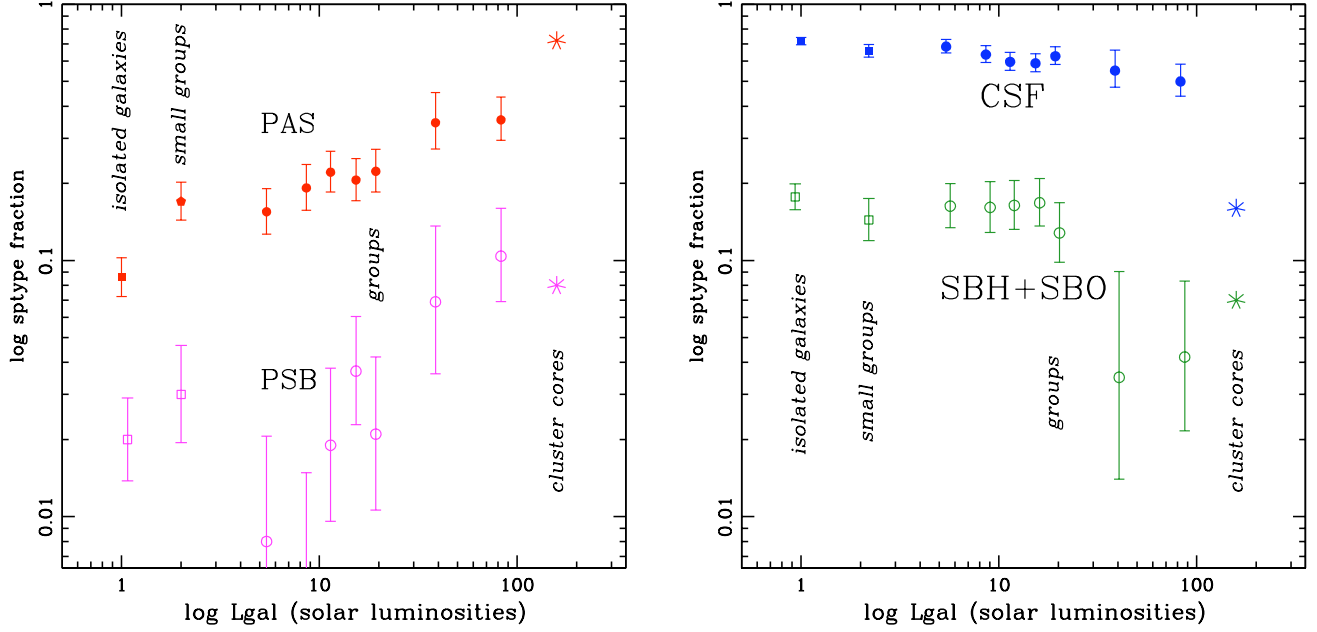


FIG. 17.— (left) The fraction of PAS and PSB galaxies across the full range of environments sampled in the ICBS, including isolated galaxies, small groups, groups, and cluster cores – some of the samples shown in Figure 14, but with averaged values for the individual samples for isolated galaxies, small groups, and cluster cores ( $R < 0.5\text{Mpc}$ ), and for binned samples of moderate-sized groups and filaments, as described in the text. Multi-component core-halo populations included in Figure 14 are omitted. The PAS (passive) fraction rises with increasing scale size of the system, which is roughly correlated with local density. The PSB (poststarburst) fraction tracks the PAS fraction, displaced lower by a factor of 10, across all environments. (right) The fraction of CSF (continuously star forming) and SBH+SBO (active starburst) galaxies across the same environments. The CSF fraction changes slowly until dropping sharply in rich groups and clusters, which is tracked by the (SBH+SBO) fraction displaced lower by a factor of 4. The plot shows that that most active starbursts, SBH & SBO, are not on the path to becoming passive galaxies: in all but the most luminous (massive) systems they are sufficiently numerous that they would overproduce the PAS galaxies (see text). Many PSB galaxies could be on the way to becoming PAS galaxies, a conclusion that is supported by the spatial concordance of the two types (see Figure 4) in the cluster environment. As discussed in the text, another and perhaps more natural interpretation of these constant ratios of PAS/PSB and (SBH+SBO)/CSF types is that the active starburst and poststarburst galaxies are hosted by CSF and PAS galaxies, respectively, which return in most cases to their previous spectral type after the burst. As discussed in the text, minor mergers and accretions are a natural way to produce this effect, even in the hotter cluster environment, where the merging of subgroups can increase the merger rate.

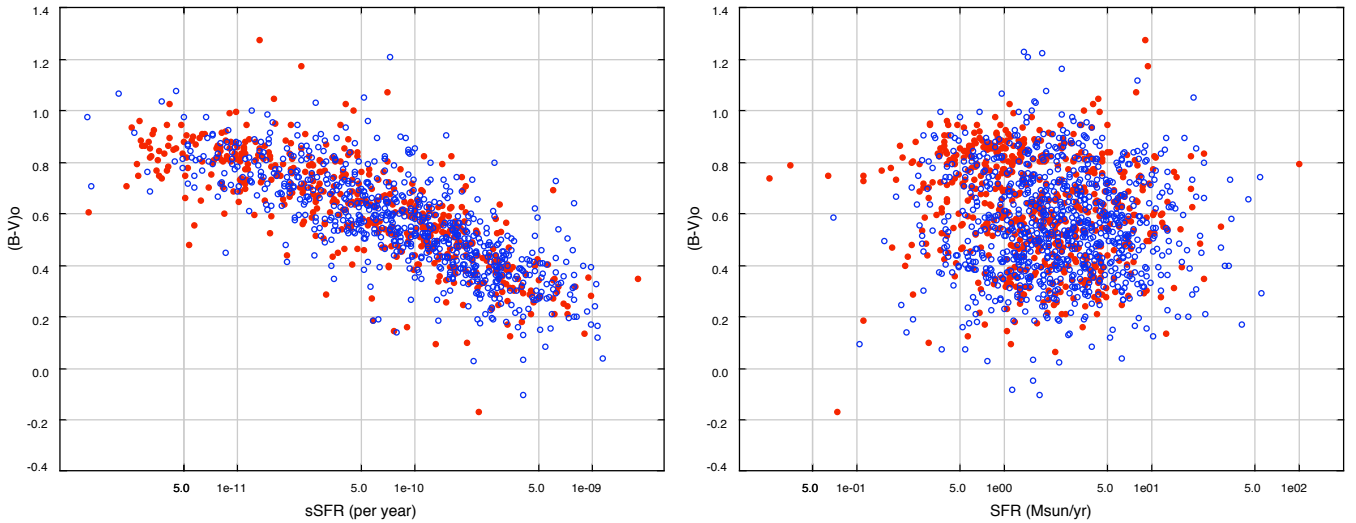


FIG. 18.— (left) The specific star formation rate (sSFR) vs rest-frame B-V color for the same 4 cluster sample as in Figure 1. (right) The star formation rate vs rest-frame B-V color. There is an excellent correlation of sSFR with color, but this relationship obscures the fact that many galaxies that are dominated by an old population have high star formation rates, as seen from the scatter plot at right. These objects could be early-type spirals forming stars continuously, or formerly passive galaxies that are experiencing an accretion/starburst event, as discussed in the text.